

MECHANISM OF ESTABLISHMENT AND BYPASS OF *IN VITRO* CELL AGING

THESIS

Presented to the Graduate Council of
Texas State University-San Marcos
in Partial Fulfillment
of the Requirements

for the Degree

Master of SCIENCE

by

Sandra Carolina Becerra, B.S.

San Marcos, Texas
August 2007

ACKNOWLEDGEMENTS

Having the opportunity to work with an exceptional professor such as Dr. Lewis has given me a greatly valued background. He has been a great mentor as well as a wonderful friend. I would like to thank you infinitely for constantly believing in me to achieve my goals. With him I evolved into a well knowledgeable individual that helped me build a strong character. This and many other qualities is what Dr. Lewis has given me. I will carry on in my career with this character that in the end will distinguish me amongst other competitive individuals.

I would also like to thank my fellow lab mates Alison, Brian, Rachel, Jennifer and Cory for the constant support and friendships that they provided. I wish you all well in your careers. Finally I'd like to thank my beloved friend Candice Gonzales who was always there every time I needed someone. Thank you all.

Aside from the gratitude from guidance in academics provided for me, I could have not accomplished this as efficiently without my mother's perseverance and great love for me. She has given me strength and courage to continue on an education. I would also like to thank my father for the support and care that he has given me throughout the years. I love you both. My last words of appreciation and love go out to my grandmother Daria Macias who always believed in my triumph. Thank you and I love you.

This manuscript was submitted on July 18, 2007.

TABLE OF CONTENTS

	Page
ACKNOWLEDGEMENTS.....	iii
LIST OF TABLES.....	v
LIST OF FIGURES	vi
CHAPTER	
I. INTRODUCTION	1
II. MATERIALS AND METHODS.....	11
III. RESULTS AND DISCUSSION.....	22
REFERENCES	60

LIST OF TABLES

Table	Page
1. <i>Saccharomyces cerevisiae</i> strains	14
2. Mating rescue of telomerase-deficient cells	33
3. Telomere fragment variations and lengths.....	54

LIST OF FIGURES

Figure	Page
1. Chromosome composition	2
2. Yeast and human telomerase complex.....	4
3. Cell cycle checkpoints	8
4. Model of the <i>EST2</i> expression system	9
5. Senescence schematic	23
6. Streak plate assay of <i>est2</i> and wildtype cells	25
7. Reactivation scheme	27
8. Plating efficiency of rescued <i>est2</i> cells.....	28
9. Yeast life cycle	30
10. Mating scheme	31
11. Holding experiment scheme	34
12. Viability of <i>est2</i> cells measured in plating efficiency.....	35
13. G ₂ arrest of X-ray damaged cells	36
14. Activation of the checkpoint response in <i>est2</i> cells.....	37
15. Picture of G ₂ arrested cells.....	38
16. G ₂ /M cell arrest.....	39
17. Plating efficiency of rescued checkpoint mutants	40
18. Viability of checkpoint mutants measured in plating efficiency	42

19. Southern blot schematic.....	44
20. Southern blot with telomere fragments of wildtype cells	47
21. Southern blot with <i>est2</i> progressive telomere shortening	48
22. Southern blot with <i>est2 mec3 rad24</i> progressive telomere shortening ...	49
23. Southern blot with telomere fragments of wildtype and rescued <i>est2</i> cells.....	50
24. Southern blot with rescued <i>est2</i> telomere fragments	51
25. Southern blot with rescued <i>est2 mec3 rad24</i> telomere fragments.....	52
26. Southern blot with rescued <i>est2 rad52</i> telomere fragments.....	53

CHAPTER I

INTRODUCTION

In humans, aging can generally be characterized by the declining ability to respond to stress, decline in body function and increased risk of disease. Because of this, death is the ultimate consequence of aging. Since cells are the fundamental structures within our bodies, the study of individual cell aging at the molecular level is important.

In eukaryotic cells, a typical chromosome is composed of a double-stranded DNA molecule coated with proteins that contains a linear array of genes that encode proteins. A schematic representation of the chromosome is illustrated on Figure 1. Eukaryotic chromosomes have specialized structures at their ends called telomeres. Telomeres are short repeated DNA sequences that are bound by telomere- and chromatin-associated proteins that form a protective cap. The telomeric region is composed of thymine- and guanine-rich sequences on one strand and adenine and cytosine-rich sequences on the complementary strand. These sequences have a potential of forming non-B form DNA structures such as intramolecular guanine-quartets (G-quartets). Adjacent to the gene-rich areas and the telomere region is the subtelomeric region that is composed of highly polymorphic and less well-defined repetitive DNA sequences.

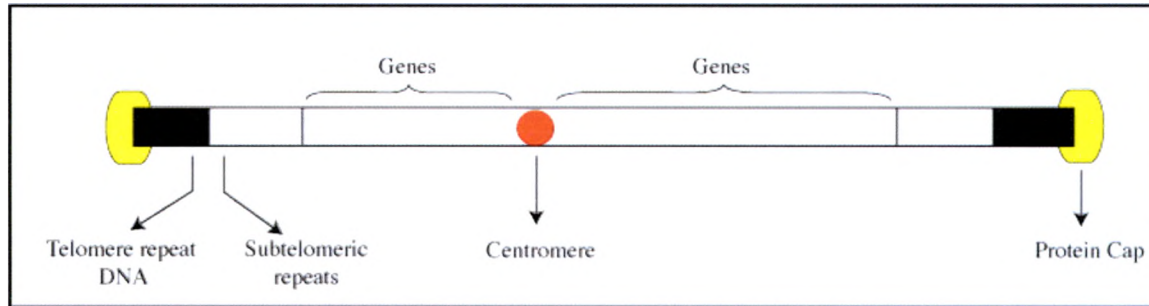


Figure 1. Illustration of the composition of a chromosome.

Conventional DNA polymerases requires an RNA primer to initiate synthesis in the 5'-3' direction. At the end of a linear chromosome, the DNA polymerases can synthesize the leading strand until the end of the chromosome. In the lagging strand, however, DNA polymerase's synthesis is based on a series of fragments, called Okazaki, each requiring an RNA primer. Without DNA to serve as template for a new primer, the replication machinery is unable to synthesize the sequence complementary to the final priming event. The result is the "end-replication problem" in which sequence is lost from the ends at each round of DNA replication (1).

The telomerase DNA polymerase enzyme holds the key to cellular aging. In human germ cells and in unicellular eukaryotes this highly conserved reverse transcriptase and its associated RNA template add telomere repeat sequences (nucleotides) to the 3' end of DNA strands by extending DNA replication during S phase. In the absence of telomerase, progressive telomere shortening occurs in the cell until cell proliferation halts (2, 3). This progressive telomere shortening is the cause of the Hayflick limit or senescence seen in cultured human cells, which divide approximately 50 times before halting growth. In humans the association of old age and chronic psychological stress has been associated to be a factor in telomere length (4). A study

done by Epel *et al.* demonstrated that increased levels of stress accelerated telomere shortening (5). Aside from stress, close correlations with telomerase reactivation in cancer cells have been observed. Over 90% of cancer cells have stable chromosome ends because telomerase expression has been reactivated (6). This is the reason why most cancer cells have found a mechanism to achieve immortality.

Human and other vertebrate telomere sequences consist of hexameric tandem repeat (TTAGGG)_n sequences. These sequences are maintained in the human germline. However, in most somatic cells, after embryonic development, human telomerase is no longer produced. For this reason human telomeres shorten as humans' age. It has been established that cells within most human tissues halt telomerase production after differentiation and subsequent display of progressive loss of the DNA repeated sequences at the ends of chromosomes (telomeres). This in turn causes the once stable chromosomes to become less stable (4, 2, 7).

One of the most studied models of cell aging is the eukaryote *Saccharomyces cerevisiae* (budding yeast). This unicellular organism has many human paralogous genes and provides multiple beneficial genetic and cell cycle characteristics that can be used for aging studies. *S. cerevisiae* cells normally produce telomerase and are immortal. Telomerase-deficient yeast cells, like human cells, undergo telomere-shortening and senescence in culture. The cause of cellular non-growth in this organism and humans is unknown. However, recent studies have indicated a specific association of mortality rates in older humans of similar age and short telomeres. Individuals that have shorter telomere lengths have higher mortality rates than those individuals with greater lengths of telomeres (4).

Telomerase-deficient yeast cells undergo telomere shortening and divide approximately 60 generations before entering a senescent phase, in which they lose the ability to replicate. As illustrated in Figure 2, *S. cerevisiae* telomerase consists of at least five subunits, including the proteins Est1, Est2, Est3 and Cdc13 as well as the *TLC1* RNA subunit. Human telomerase shown at the right side of the figure, has a similar composition. Est1 and Cdc13 are single-stranded DNA binding proteins that may target telomerase to 3' overhang structures found at chromosome ends during S phase. Est2 is the catalytic component of the complex. Est3 has an unknown function and *TLC1* is the RNA subunit (3). *TLC1* contains an internal 17 nucleotide sequence (CACCACACCCACACACA) that is used as a template by the enzyme to synthesize new telomeric DNA repeats. Yeast cells that have mutations in the *EST1*, *EST2*, *EST3* or *TLC1* genes exhibit progressive telomere shortening, cellular senescence and eventual inhibition of cellular growth (8).

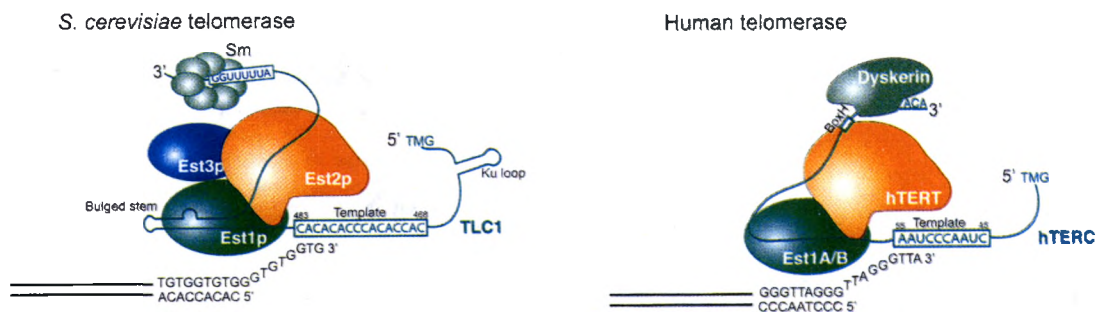


Figure 2. Illustration of the telomerase demonstrating similar composition in both the *S. cerevisiae* and human complexes (9).

In culture, a small fraction of cells called “survivors” appear in late phases of senescent cell cultures. An explanation for survivor mutant cells is that these cells have bypassed senescence by replenishing their chromosome ends through enhanced homologous recombination at telomeres (10).

Models that have been proposed to explain senescence are the following: first cells may form lethal chromosome rearrangements such as end-to-end chromosome fusions as DNA ends become uncapped and more reactive. Second, chromosomes may lose essential genes from the ends as shortening eventually proceeds past the telomeres. Other models that have been proposed include apoptosis (programmed cell death) whereby cells become committed to inevitable death, or alternatively, cells may simply arrest growth in G₂ phase (dependent on checkpoint genes *MEC3*, *RAD24* and other DNA damage response genes) (11, 12). In this last model, cells remain viable and do not actually die during senescence, but have the ability to sustain viability for a prolonged period of time though they are not growing (13, 7, 14, 12, 15, 16).

In the study of cellular aging, it has been accepted that the lack of the telomerase enzyme is a strong factor affecting the lengths of chromosomes. However, there are other contributing factors that may aid in decreasing chromosome lengths. These factors include naturally occurring reactive oxygen species (ROS) that can produce accumulation of oxidized nuclear and mitochondrial DNA and have been noted to appear during aging (17). Oxidative DNA damage can ultimately lead to telomere instability and chromosome loss. ROS include hydroxyl radicals, peroxides and superoxide anion free radicals. They are molecules that are highly reactive due to the presence of unpaired electrons. Cells are normally able to defend themselves against ROS damage through the

use of antioxidants such as superoxide dismutase and glutathione peroxidase and catalases. (18, 19). In a study done by Chen *et al.* (1995) human diploid fibroblast cells were used to identify a correlation between increased levels of oxidative DNA damage, using 8-oxo-2'-deoxyguanosine (8-oxoG), and senescence. The results demonstrated an increased oxidant "hit rate" in senescent cells compared to young cells (20). Oxidation of DNA or nucleotides generates 8-oxoG, which allows guanine to pair aberrantly with adenine, causing GC to TA transversion mutations if not repaired.

Conversely, treatment of cells with antioxidants has been proven to slow the process of senescence by reducing intracellular oxidative damage (21). Antioxidant molecules are able to terminate oxidative chain reactions by removing radical intermediates and inhibiting other oxidation reactions by oxidizing themselves. Such molecules include glutathione, vitamin C and vitamin E. An experiment performed by Yokoo *et al.*, demonstrated the effects of ascorbic acid (vitamin C) in neonatal human epidermal keratinocytes. This study revealed that ascorbic acid and other glycosylated or phosphorylated derivatives can reduce intracellular ROS and consequently increase cell longevity (21). Serra *et al.* (2003) performed a study that used human fibroblast cells that expressed senescent-like growth arrest when exposed to mild oxidation. After treatment with superoxide dismutase linked to a metal and other mimetics they observed a reduction in the rate of telomere shortening and extension of the replicative life span of cells (22).

Senescence *in vitro* is caused by the lack of either the RNA component (*TLC1*) or a protein component (such as *EST2*) of telomerase. Cells with these genes deleted exhibit progressive telomere shortening (23). In *S. cerevisiae*, when telomeres reach a short

length, mitotic recombination is activated through the *RAD52* gene to stabilize or lengthen telomeres by increasing strand exchange events at the telomeres (12). *RAD52* is essential for repair of double-strand breaks (DSBs), which is a crucial function for maintaining chromosome and telomere integrity (23). The repair of DSBs is a function that is associated with two pathways. One pathway involves homologous recombination in the cell cycle. The other major pathway allows for direct rejoining of broken ends and is called non-homologous end-joining (24). Genes in the *RAD52* group are *RAD50*, *RAD51*, *RAD52*, *RAD54*, *RAD55*, *RAD57*, *RAD59*, *XRS2* and *MRE11* (23). *rad52 tlc1* double mutant yeast strains progress through senescence at a faster rate than *tlc1* single mutants (23). This is an indication that the rate of senescence is influenced by the deletion of genes essential for DSB repair.

Cell cycle checkpoint mutants also play a critical role in senescence. Checkpoints are mechanisms that delay the continuation of the cell cycle at certain points to “check” whether the cells are ready to proceed further and become activated before proceeding to the next event (25, 26). In *S. cerevisiae* the major pause point caused by the presence of damaged DNA is in G₂ (Figure 3). This G₂/M checkpoint pauses cycling to give cells time to repair the damage before attaching the chromosomes to the spindle and pulling them apart during M phase.

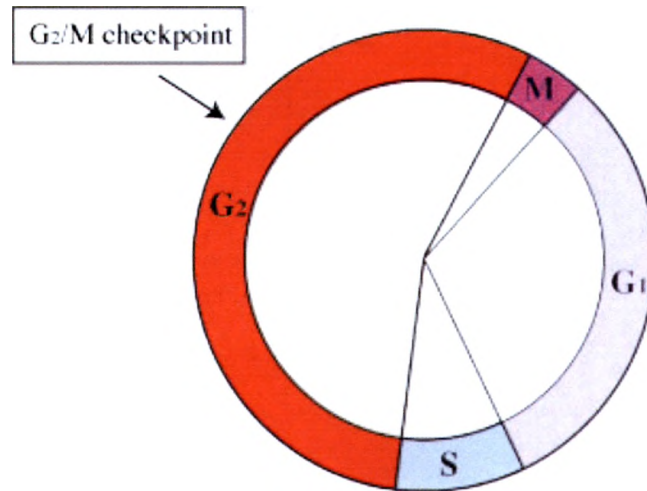


Figure 3. Illustration of the major DNA damage-response cell cycle checkpoint in *S. cerevisiae*.

In *S. cerevisiae*, *RAD9*, *RAD17*, *RAD24*, *MEC3*, *DDC1* and *DDC2* sensor genes are required to recognize the presence of damaged DNA and activate the checkpoint. This cell cycle arrest is activated in response to DNA damage leading to pausing of the cycle for long enough to repair the damage before resumption of cycling. When this checkpoint mechanism fails, cells continue to divide with damaged chromosomes. Several genes involved in the DNA damage checkpoint are also involved in telomere length maintenance. Studies conducted by Ijpma and Enomoto *et al.* demonstrated that checkpoint arrest occurs during senescence, causing cells to arrest in G₂/M (12, 11). This response is due to telomere shortening and uncapping. Cells that were deficient in checkpoint pathway genes *rad24* or *mec1* did not exhibit G₂ arrest during senescence.

The current thesis project has attempted to understand the mechanism by which these senescing cells stop dividing and determine if there is a way to revive already

senescent cells. Characterization of factors affecting the establishment and bypass of replicative senescence has permitted an investigation of the mechanism of cellular growth inhibition during aging. A plasmid with a regulatable Est2 polymerase expression system, under the control of a galactose-inducible promoter (*GAL1-V10p::EST2*), was developed in the laboratory to study cell aging and can be seen in Figure 4.

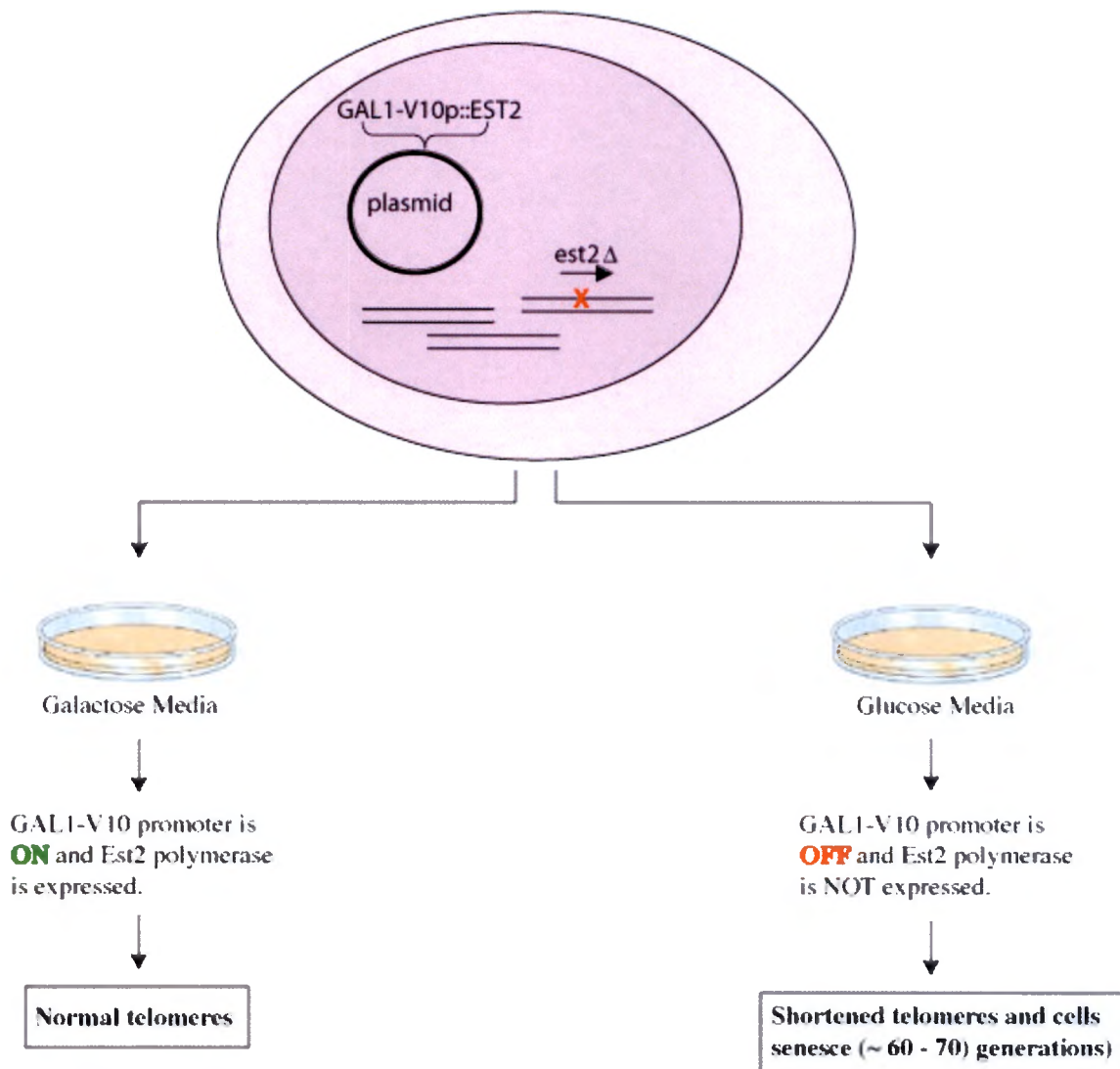


Figure 4. Illustration of the Est2 polymerase expression system indicating the activation (galactose media) or deactivation (glucose media) of telomerase.

This expression system allows for manipulation of telomerase expression in cells by using media containing galactose (Est2 polymerase synthesis remains on) or glucose (Est2 polymerase remains off). When cells containing this plasmid are placed on glucose media, telomerase is no longer expressed and cells undergo progressive telomere shortening and are destined to halt cellular growth after approximately 60 generations (27). Using this expression system, it is possible to study senescence in various strains of *S. cerevisiae*. The current study relied on this expression system to manipulate the reversibility of senescence to critically test previously proposed mechanisms for *in vitro* cell aging.

CHAPTER II

MATERIALS AND METHODS

I. MATERIALS

General reagents

Sodium chloride and sodium dodecyl sulfate were purchased from Mallinckrodt AR (Paris, KY). Agarose, tween 20 and sarkosyl were obtained from Sigma-Aldrich Chemical Co. (St. Louis, MO). Sodium acetate was purchased from Mallinckrodt Baker, Inc. (Paris, KY). Trizma-base was purchased from VWR International (West Chester, PA). Ethidium bromide and Tris-HCl were purchased from Shelton Scientific (Shelton, CT). Maleic Acid and formamide were both obtained from Fisher Biotech (Fair Lawn, NJ). Sodium hydroxide and Sodium Citrate were purchased from Merck, (Darmstadt, Germany).

Yeast growth media

All amino acids, D-(+)-glucose, and ampicillin were purchased from Sigma-Aldrich (St. Louis, MO). Bacto peptone, bacto yeast extract, bacto tryptone and bacto agar were obtained from Becton Dickinson Microbiological Systems (Sparks, MD). D-(+)-galactose was purchased from Pfanstiehl Laboratories, Inc. (Waukegan, IL) and also from Sigma-Aldrich (St. Louis, MO).

Enzymes and PCR reagents

Restriction enzyme *XhoI* was purchased from New England Biolabs (Beverly, MA). DNA polymerases Taq DNA polymerase, Vent DNA polymerase and Vent (exo⁻) DNA polymerase were purchased from New England Biolabs (Beverly, MA). Taq DNA polymerase was also purchased from Fermentas (Hanover, MD). Herculase II fusion DNA polymerase was obtained from Stratagene (La Jolla, CA).

Cell culture solutions and media

General growth media where cells were grown as YPDA. This media contained 1% bacto yeast extract, 2% bacto peptone, 2% glucose, and 2% bacto agar. For plasmid selection, yeast cells were grown on synthetic media with drop-out mix (2% glucose or 2% galactose and 2% bacto agar, plus all essential amino acids and bases exempting those used for plasmid selection). All quantities listed as “%” are w/v here and elsewhere. Synthetic media plates for senescence assays used 2% glucose, 2% bacto agar and all the essential amino acids and bases exempting those required for plasmid selection. Mating rescue synthetic media plates were prepared using 2% galactose, 2% bacto agar and excluded amino acids leucine, histidine, tryptophan and adenine. Senescence reactivation and holding experiments required synthetic media plates using 2% glucose or 2% galactose growth media. YPDA or YPGal used in either the mating rescue or the reactivation rescue of cells included 1% bacto yeast extract, 2% bacto peptone, 2% bacto agar and either 2% glucose or galactose, respectively.

Yeast strains and plasmids

The parent strains used for these studies were derived from BY4742 (*MATa his3Δ1 leu2Δ0 lys2 Δ0 ura3Δ0*) and are listed in Table 1 (28). The *est2* strain utilized in all initial assays was YLKL803 (BY4742, $\Delta est2::HygB'$ containing plasmid pLKL82Y [*CEN/ARS URA3 GAL1-V10p::EST2*]). For testing senescent cells that were rescued through mating, the *est2*- YLKL803 strain was mated to YLKL701 (*MATa ade5⁻*). Reactivation experiment strains included YLKL803, checkpoint mutants YLKL840 (YLKL803, $\Delta rad24::G418'$), YLKL841 (YLKL803, $\Delta mec3::G418'$) and checkpoint double mutant YLKL844 (YLKL840, $\Delta mec3::Nat'$). The holding experiment used the telomerase-deficient strain YLKL803 and checkpoint double mutant strain YLKL844. Analysis of telomere lengths using a Southern blot assay required the use of a probe containing plasmid YTCA-1 (29). Strains included in this experiment were YLKL803, YLKL844 and YLKL807 (YLKL803, $\Delta rad52::G418'$).

Yeast strains and plasmids

All yeasts strains and plasmids used in this study are listed in Table 1.

Table 1. *Saccharomyces cerevisiae* strains

Strain	Genotype	Reference
BY4742	<i>MATα his3Δ1 leu2Δ0 lys2Δ0 ura3Δ0</i>	(30)
YLKL701	<i>MATα ade5</i>	Lab strain
YLKL803	BY4742, Δ <i>est2</i> <i>HygB^r</i> + pLKL82Y (<i>GAL1-V10p EST2, URA3</i>)	(27)
YLKL807	YLKL803, Δ <i>rad52</i> <i>G418^r</i>	Lab strain
YLKL840	YLKL803, Δ <i>rad24::G418^r</i>	Lab strain
YLKL841	YLKL803, Δ <i>mec3::G418^r</i>	Lab strain
YLKL844	YLKL840, Δ <i>mec3::Nat^r</i>	Lab strain

II. METHODS

Chromosomal and plasmid DNA purification

Extraction and purification of chromosomal DNA was performed using the Master Pure Purification Kit provided by Epicentre Technologies. The protocol was followed as recommended by the manufacturer.

Fluorometry assay

After DNA purification, the DNA concentration was quantified using a Hoefer DyNA Quant 200 Fluorometer system (Amersham Pharmacia Biotech). The protocol required the use of standard calf thymus DNA for calibration and assay buffer A (0.1% Hoechst 33258 and 5% 10x TNE containing 0.2 M NaCl, 10 mM Tris-Cl and 1 mM EDTA at pH 7.4).

Solid media-based senescence assays

Cell senescence was observed by streaking telomerase-deficient and wildtype control cells from the low colony density regions of a freshly streaked Gal-Ura stock plate using sterile toothpicks onto YPGlu (rich) or synthetic Glu-Ura plates. These cells were grown for two days (YPGlu) or three days (synthetic Glu-Ura) at 30 °C. After the first streak, cells were re-streaked from moderate-sized individual colonies onto a fresh YPGlu or Glu-Ura plate again and the process was repeated until senescence occurred after approximately four streaks. The senescing cells were defined by their loss of the ability to grow compared to the wildtype control cells that would grow indefinitely. The apparent senescent phenotype was visible by the fourth streak in BY4742 cells and the third streak in certain DNA repair mutant strains (~60-80 generations). Images of each streak were captured using a Canon Powershot G3 digital camera and saved as .jpg formatted files. The

plate senescence assay was followed to test cellular senescence in all the mutant strains and to observe any possible senescence rescue following the methods below.

Senescent cell mating rescue experiment

To determine the efficiency of rescuing senescent cells by mating parent strains (*MAT α* BY4742) or Δ *est2*-BY4742 mutant cells containing the plasmid pLKL83Y ([*CEN/ARS URA3 GAL1 V10p::EST2*]) were propagated on galactose plates containing all the essential amino acids and bases required for proper growth. Similarly, the mating type tester strain YLKL701 (*MAT α*) was streaked on YPDA plates until it was used. Cells were grown at a temperature of 30 °C for two to three days. *MAT α est2* cells were then re-streaked onto fresh glucose plates three times to drive the cells to a point of senescence. *est2* cells that were near senescence and the *EST2* control parent strain BY4742 were then harvested using a sterile toothpick and placed in 2 ml YPDA broth. An incubation period of approximately 60 minutes at 30 °C was established prior to mating to allow the cells to reach log phase. After the incubation period, cells were diluted, sonicated and counted using a hemacytometer. Equal ratios of the strains were mixed in a tissue culture flask for mating of YLKL803 (*MAT α est2*) x YLKL701 (*MAT α EST2*) and BY4742 (*MAT α EST2*) x YLKL701 (*MAT α EST2*). The mating period lasted 120 minutes at 30 °C. Cells were then diluted and spread to galactose plates and to diploid selective Glu-leu-his-trp-ade plates to identify formation of diploids. The rescue efficiency was calculated by doing plating efficiency counts, which is defined as the number of cells able to form colonies on plates divided by the number of cells in the culture counted microscopically.

EST2 reactivation assay

Initial *EST2* reactivation studies were done by streaking *est2* cells containing the *GAL1-V10::EST2* plasmid pLKL83Y (strain YLKL803) from a fresh galactose plate to a glucose plate that lacked uracil. Cells were grown for three days at 30 °C (approximately 20 generations) before restreaking onto a fresh glucose plate and growth for three more days. The third streak was allowed to grow four days, as was the fourth streak, which was sometimes streaked heavily as a patch. From the third streak, colonies were harvested, diluted, sonicated and counted using a hemacytometer. Fourth streak colonies were also harvested and counted. Cells were spread to glucose plates and also to galactose plates to determine whether late senescent cells could be rescued by reactivation of telomerase expression. The colony forming ability of cells was tested by measuring the plating efficiency.

Later, reactivation experiments involving checkpoint single and double mutants (*mec3*, *rad24*, and *mec3 rad24* cells) were performed to compare their survival rates to those of checkpoint-proficient strains. These mutants were streaked on glucose plates using the normal senescence assay. After the third streak, colonies of each mutant were harvested, sonicated, counted, diluted and spread to glucose and galactose plates to determine whether late senescent cells lacking either or both essential checkpoint genes could be rescued efficiently using the telomerase expression reactivation system.

Senescent cell holding experiment

Telomerase-deficient *est2* cells along with the double mutant strain YLKL844 (*mec3 rad24*) were streaked onto glucose plates for the first and second streaks as before. After cells had undergone ~ 40 generations in the two streaks, seven colonies were harvested into 500 µl of water and counted separately as mentioned previously. Volumes were calculated to spread cells for the third plate, instead of streaking, in order to get well-separated colonies. The cells grew for three days before harvesting seven colonies into water and

spreading dilutions onto both galactose and glucose plates without uracil to monitor the rates of reactivation. The original third growth plate (similar to a third streak) was placed back into the 30 °C incubator. After two more days, seven colonies were harvested again, counted and spread to galactose and glucose plates as done previously. The original third plate was placed back into the 30 °C incubator once again and the same process of harvesting, counting and spreading to galactose and glucose plates was repeated three more times, every two days. Ultimately, the third growth plate was held in the incubator for eight consecutive days.

Southern blot experiment

PCR amplification of nonradioactive DIG probe. Probes for Southern analysis were synthesized by PCR. Eight reactions were performed using a prep of plasmid YTCA-1 that was diluted 1/100 for all reactions. One microliter of miniprep template DNA, 5 µl primer M13 forward (5'-AGCGCGCAATTAACCCTCACTAAAG-3'), 5 µl primer M13 reverse (5'-CAGGAAACAGCTATGACC-3'), 5 µl 10X PCR buffer with MgCl₂, 5 µl 10X PCR DIG labeling mix (2 mM dATP, 2 mM dCTP, 2 mM dGTP, 1.3 mM dTTP, 0.7 mM Digoxigenin-11-dUTP) and either 1 µl Taq DNA polymerase, Vent (exo⁻) DNA polymerase, Vent DNA polymerase or Roche Expand High Fidelity mix enzyme were combined with sterile double distilled water to bring each reaction to a final volume of 50 µl. An unlabeled DNA control was run and the reaction contained all of the same additions as mentioned above only no DIG labeling mix was added. A kit control PCR was also run and varied from the initial reactions described only by the addition of a control template DNA in place of YTCA-1 template DNA. The reactions were then exposed to the following thermocycler conditions: 94 °C, 2 min. and then 32 cycles: 94 °C, 30 sec., 40 °C, 30 sec., 72 °C, 1 minute., followed by extension of all

unfinished strands at 72 °C for 7 min. The PCR samples were run on a 2.2% agarose gel, stained with ethidium bromide and visualized on a Kodak Image Station 440 instrument.

DNA isolation and purification. Senescent cells that had been rescued via the telomerase expression system were harvested from colonies on galactose plates lacking uracil and placed in three ml overnight cultures of YPGal broth and grown overnight in a 30 °C shaker. The DNA was then purified using the MasterPure™ Purification Kit from Epicentre. After purification, DNA concentrations were quantified by fluorometry.

Southern blot agarose gels require at least one to two µg of DNA to be loaded. Therefore, three to four µg of DNA was digested overnight with restriction enzyme *Xho*I at 37 °C. The digested DNA was then concentrated by ethanol precipitation and again quantified by fluorometry. One µg of each sample was loaded onto a 1.2% agarose gel. Gel electrophoresis conditions involved running at 130 volts for 5-10 minutes and then at 100 volts for the remainder of the run. The gel was stained in ethidium bromide for 10 minutes and analyzed using a UV transilluminator to confirm that digestion was complete.

DNA denaturation and neutralization. After staining each gel was washed for five minutes with denaturation buffer (8.7% sodium chloride, 2% sodium hydroxide) and then again for 30 minutes at room temperature. Next, the gel was washed in neutralization buffer (8.7% sodium chloride, 6.1% Tris base) for five minutes and then again for 30 minutes at room temperature. The DNA from the gel was transferred overnight onto an N+ Hybond membrane using a homemade capillary transfer apparatus. Once overnight transfer was complete, the DNA was crosslinked to the membrane in a UV-Stratalinker 2400 (Stratagene) at 120,000 microjoules for ~20 seconds.

Probe Hybridization. For prehybridization, the membrane was rotated in a glass roller bottle in 15 ml of prehybridization/hybridization solution (50% v/v formamide, 5X SSC, 0.1% sarkosyl, 0.02% SDS, 1X blocking agent from Roche) for one hour at 40 °C. A dilute 5X SSC buffer was prepared from 20X SSC stock solution (35.1% NaCl and 17.6% sodium citrate). The 15 ml of prehybridization solution was poured off and replaced with 15 ml of fresh prehyb/hybridization solution. One hundred microliters of denatured digoxigenin (DIG)-labeled probe was added to the tube. The DNA probe was denatured by placing it in 50% formamide solution and heating at 100 °C for five minutes and followed by transfer to wet ice for two minutes. The membrane in solution was rotated in a roller bottle overnight at 40 °C.

Detection by chemiluminescence. The blot was removed from the overnight tube and placed in a solution of 2X SSC/0.1% SDS and shaken at room temperature for five minutes twice. The blot was then washed twice for five minutes each in 0.5X SSC/0.1% SDS at room temperature. The membrane was then equilibrated in washing buffer (0.1 M maleic acid, 0.15 M NaCl, 0.3% Tween 20 v/v; pH 7.5) for one minute, which was poured off and replaced by fresh washing buffer. After another minute, the washing buffer was poured off and 100 ml of 10X blocking solution (180 ml of maleic acid and 20 ml of Roche blocking solution) was added, followed by shaking for 30 minutes. The blocking solution was then poured off and 30 ml of enzyme-linked antibody solution (six μ l antibody solution from Roche in 30 ml 1X blocking solution) was added and the blot was left to shake for 30 minutes. The antibody solution was poured off and the blot was washed twice with 100 ml wash buffer for 15 minutes each. This solution was poured off and the blot was incubated for two to five minutes with 20 ml of detection buffer (0.1M

tris-HCl, 0.1 M NaCl; pH 9.5). The blot was removed from the buffer and placed into a clear plastic bag. One milliliter of enzyme substrate, disodium 3-(4-methoxyspiro(1,2-dioxetane-3,2'-(5'-chloro)tricyclo[3,3.1.1^{3.7}]decan}-4-yl) phenyl phosphate (CSPD), from Roche Diagnostics was added directly onto the membrane in the bag. The bag was immediately closed and the substrate solution was spread evenly over the surface of the membrane. The membrane was allowed to incubate at room temperature for five minutes before all of the liquid was squeezed out of the bag. The bag was then sealed. The blot was incubated at 37 °C for 10 minutes. For imaging, the membrane was placed in an X-ray cassette with one sheet of 8 x10 cm Kodak Biomax MR film. Exposure times for each film varied from 25-120 minutes before development.

CHAPTER III

RESULTS AND DISCUSSION

Preservation of youth and health is a major concern in the world today. As people age, their bodies begin to deteriorate, organs become less efficient and risk of diseases upsurges. Understanding and exploring these concerns is the reason why a great deal of scientific research has focused on human aging. This research project has explored the fundamental elements and has tried to understand the mechanism of cellular senescence using the model organism *S. cerevisiae*. The primary cause of senescence or aging in cultured cells is the absence of the telomerase complex in the cells. In humans, telomerase enzyme activity is absent in most normal cells. However, the enzyme is active in germ and stem cells. It has been established that normal human cells progressively lose telomeric DNA *in vivo* and also with passage in cell culture due to the lack of telomerase. As can be seen in Figure 5, DNA sequences at the ends of chromosomes are lost progressively, potentially resulting in loss of the protein cap that protects the ends from degradation and unwanted chemical reactions. Therefore, absence of the enzyme telomerase leads to various consequences in the cell, a few of which are shortening of the telomeres at the ends of chromosomes, loss of the protective protein caps, inhibition of cell growth, and ultimately to loss of cell viability. Accumulation of these events in a cell is what is recognized as cellular senescence.

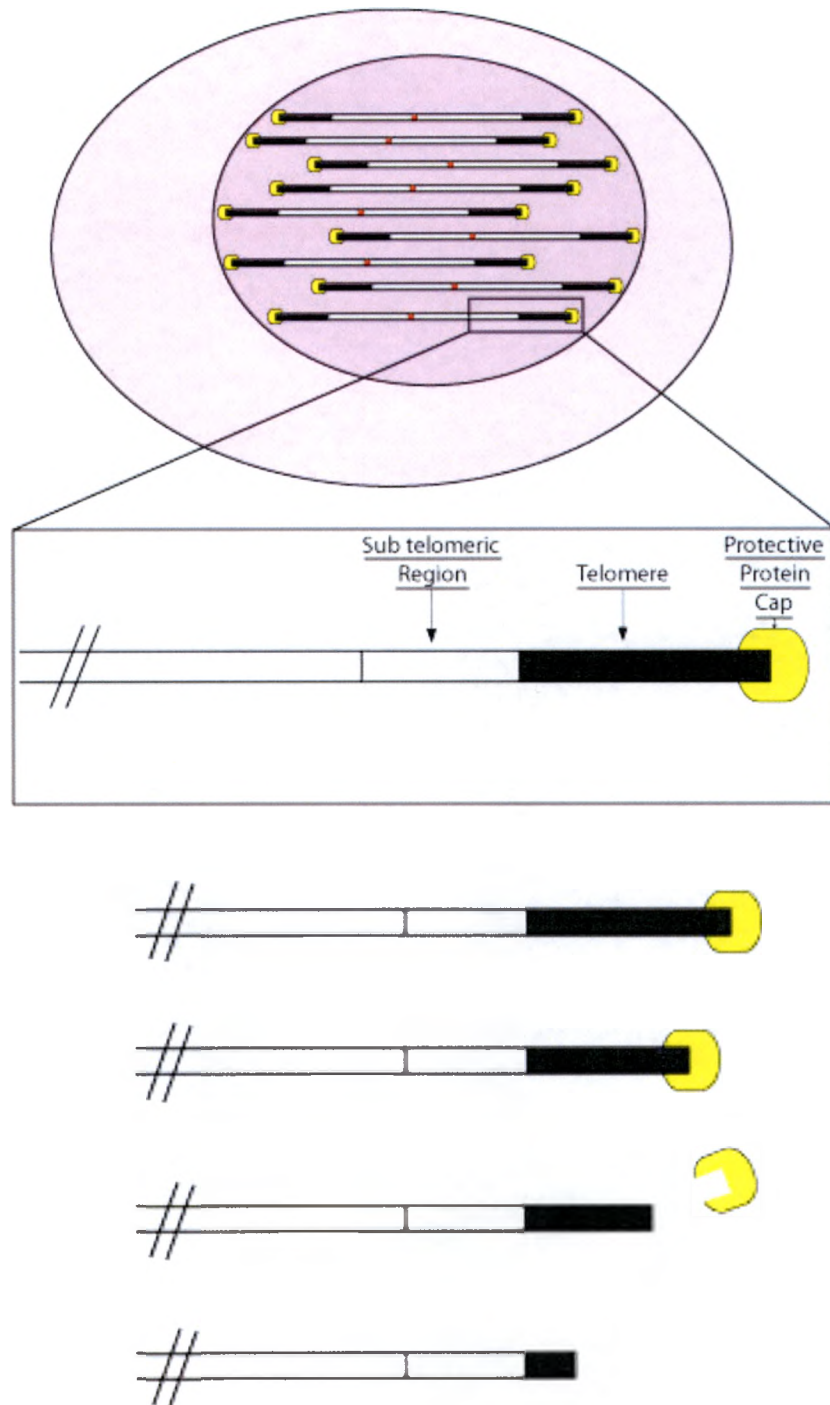


Figure 5. This schematic depicts telomere shortening and uncapping processes thought to occur *in vivo* and in cultured human cells.

Several models have been proposed to explain why humans and other eukaryotic cells grown in culture have a finite lifespan. For example, cells may form lethal chromosome rearrangements such as end-to-end chromosome fusions or the chromosomes may ultimately lose essential genes from the ends. Another model suggests that telomere shortening may initiate an irreversible process that leads to death called apoptosis. Alternatively, the possibility that cells may simply arrest growth, without commitment to cell death, may be occurring.

This research project has employed the budding yeast *S. cerevisiae* as a model system to critically test previously proposed models of cell aging. To explore senescence, we have used a special yeast strain created in Dr. Lewis' lab that has the polymerase subunit of telomerase, *EST2*, under the control of an inducible promoter *GALI-VI0* (27). This sophisticated expression system, shown schematically in Figure 4 (see Figure 4 in Chapter 1), has the advantage that it is possible to modulate expression of telomerase inside cells. For example, when the cells are grown on plates or in liquid media that contains the sugar galactose, the *EST2* polymerase is expressed and cells are immortal. Conversely, when cells are placed onto media containing glucose, the *GALI-VI0p::EST2* gene is turned off and cells can only grow for approximately 60-70 generations (or cell cycles) before halting proliferation. Figure 6 shows the progressive decline of cell proliferation as cells advance through generations in telomerase-deficient cells versus cell viability maintenance in telomerase-proficient cells. In this assay, streaked cells grow through approximately 20 generations on the surface of a plate to form a colony. Cells from the colony are then re-streaked to a fresh plate, where they form colonies that have undergone approximately 40 cell cycles. After cells from these

colonies are streaked again (the third streak in Figure 6), they grow an additional 15-20 generations prior to a fourth streak. At this point the senescing cells have grown for about 60 generations and cannot form normal colonies on this final plate.

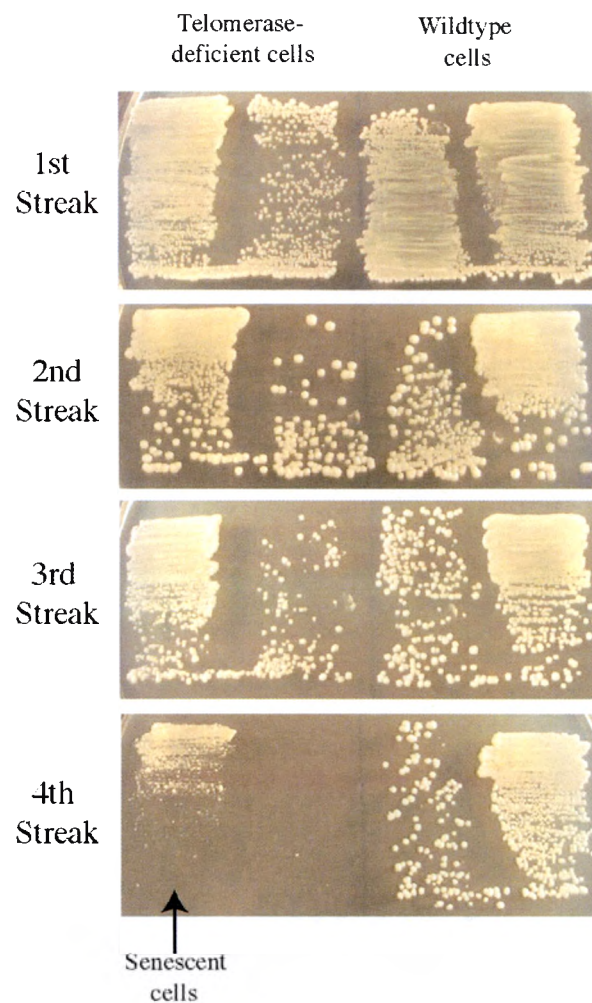


Figure 6. Illustration of senescence in telomerase-deficient (*est2*) cells compared to normal growth of the wildtype strain (BY4742).

Senescence models such as those involving creation of end-to-end chromosome fusions or degradation of DNA ends until critical genes are lost propose that senescence is essentially an irreversible process. Thus according to these models, cells that have

progressed to late senescence (60-70 generations) cannot be rescued by simply reactivating telomerase and allowing it to replenish the telomere sequences lost from the ends of each chromosome.

To test the models of senescence, an experiment was designed to test if in fact cells become irreversibly committed to die during senescence. This experiment involved the use of the *EST2* polymerase expression system to study the consequences of reactivation of telomerase in telomerase-deficient cells. If cells that had entered a late senescent phase and had accumulated DNA damage could be rescued by reactivation of telomerase, then this would contradict some of the speculated models of senescence suggesting irreversible cell death, for example apoptosis, chromosome fusions or gene deletion. The experiment was initiated by streaking telomerase-deficient (*est2*) cells on a glucose plate at 30 °C and re-streaking them until they underwent cellular senescence. When these cells had reached a near-senescent phase (~ 60-70 generations), they were harvested, transferred into water, counted in a light microscope and spread to glucose plates (*Est2* remains off) and to galactose plates (*Est2* is turned back on) and again placed at 30 °C. Figure 7 displays the experimental approach that was used.

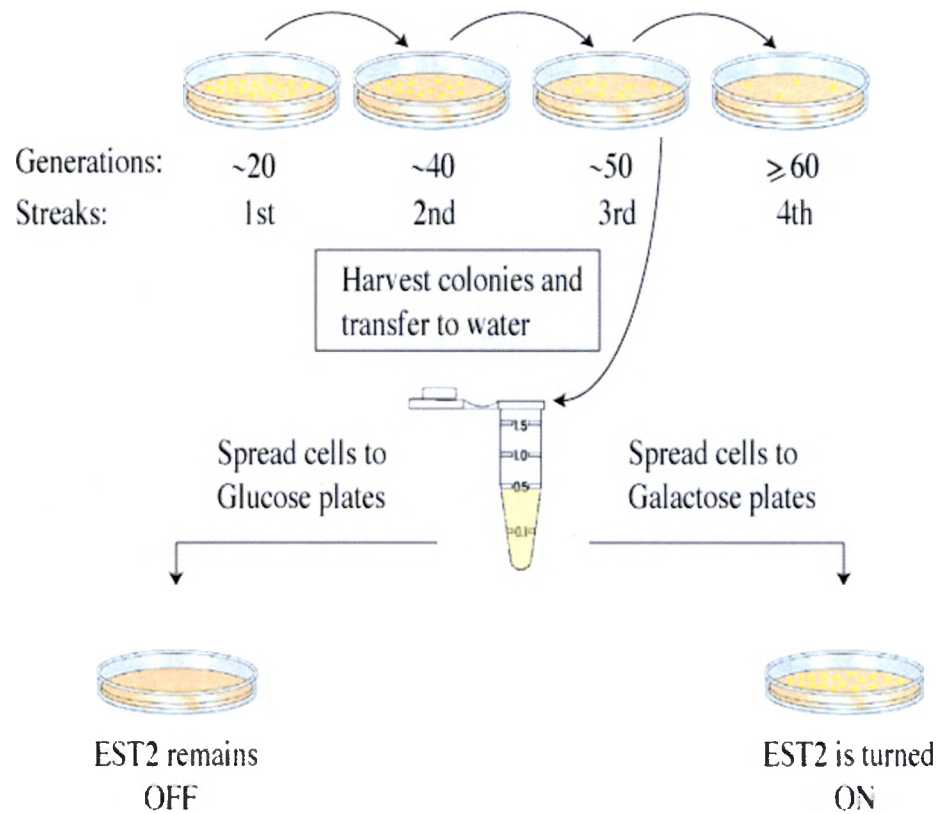


Figure 7. Visual description of the approach used to determine whether reactivation of telomerase expression rescues non-growing, senescent cells and allows them to resume cycling and form colonies on galactose plates.

Results of this experiment using the telomerase-deficient *est2* yeast strain are shown in Figure 8. This graph demonstrates that cells that had stopped growing in late senescence could in fact be rescued by turning telomerase back on. As shown in the figure, normal wildtype cells have plating efficiencies of $> 70\%$ on both glucose and galactose plates. Plating efficiency is defined here as the percentage of total cells in a culture that are able to form colonies when spread onto a Petri dish. As expected, when late senescent cells were spread to glucose plates, keeping telomerase expression off, $> 99\%$ of the cells could not form colonies, i.e., plating efficiency was only 0.5% . In

contrast, when these same cells were spread onto galactose plates, turning telomerase back on, the non-growing cells began cycling again and 44% of the cells were able to form colonies. This represents a 92-fold increase upon reactivation of the *EST2* polymerase.

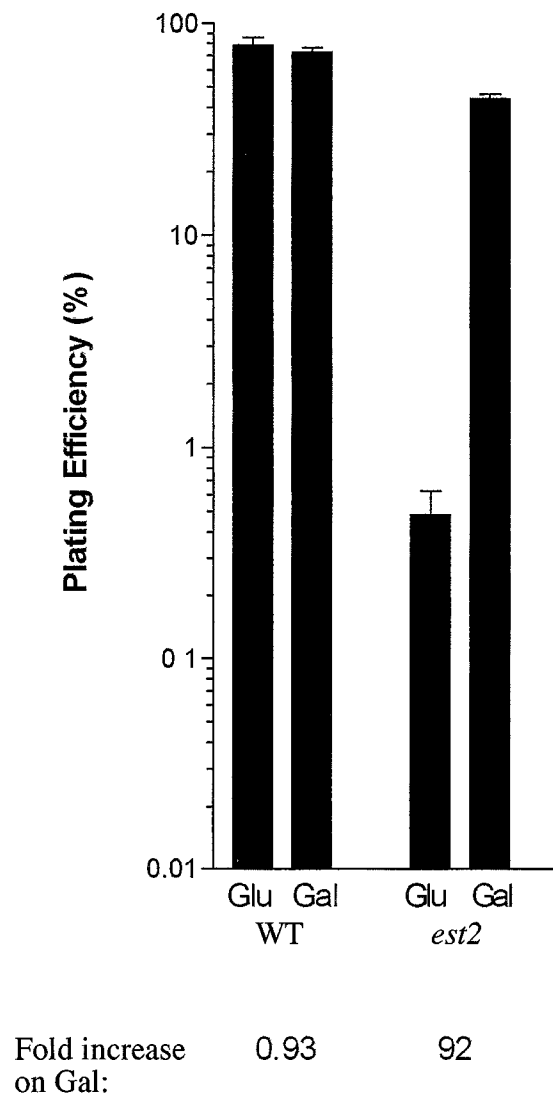


Figure 8. Efficiencies of colony formation for wildtype (WT) and late senescence *est2* cells containing a *GALIV10p::EST2* fusion on glucose and galactose containing plates. Error bars indicate standard deviations.

In addition to the reactivation experiment, an alternative experiment was conducted to once again assess the reversibility of senescence. This experiment employed the concept of DNA complementation through yeast mating. The experiment was designed to address if non-growing telomerase-deficient haploid cells in late senescent phase would resume growing if they could be mated (fused) with telomerase-proficient haploid cells to form stable diploids.

In the yeast life cycle, (Figure 9), when diploid cells (called *MATa* /*MATα*) enter a starvation mode, they undergo meiosis, creating haploid spores that can germinate and grow as haploid cells (31). These haploid cells can also later mate and reform diploids by a process involving cell signaling receptors and pheromones. The process of mating haploid yeast cells to form a stable diploid is illustrated in Figure 10. This figure depicts the theory of rescuing a telomerase-deficient cell in late senescent phase by mating it to a telomerase-proficient cell.

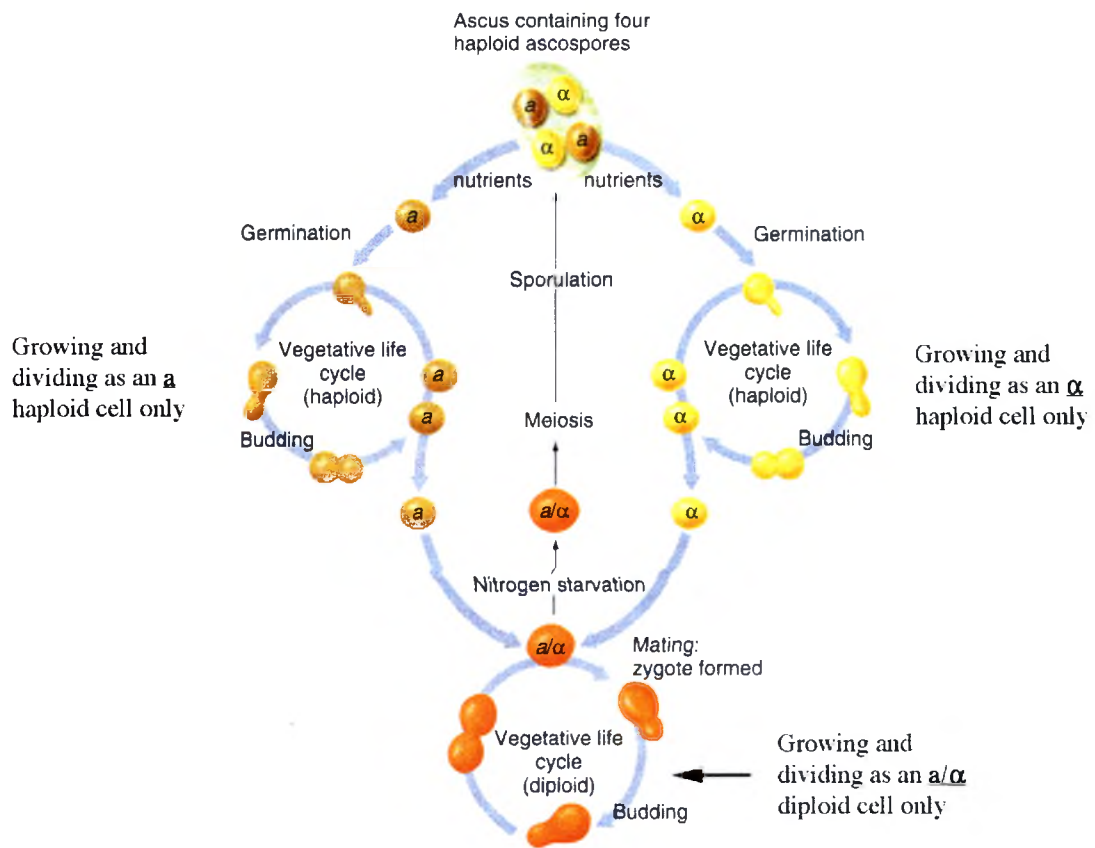


Figure 9. This image outlines the lifecycle of haploid and diploid yeast cells (32).

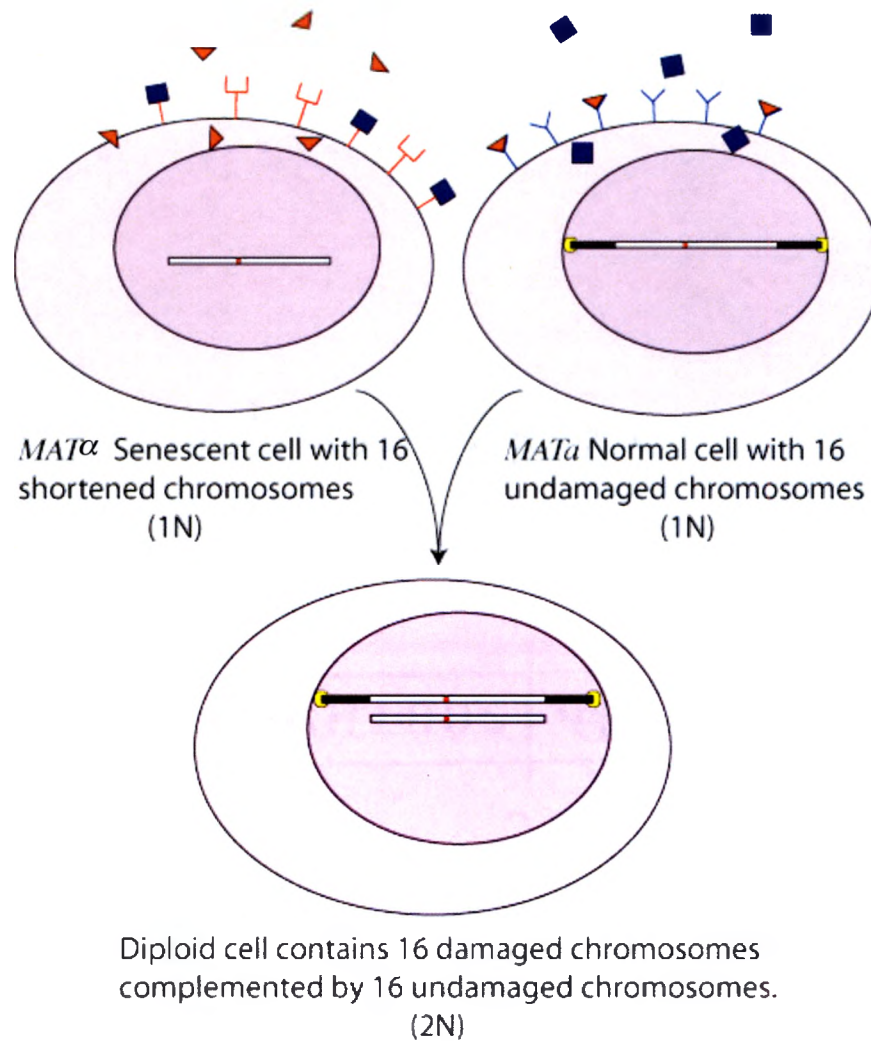


Figure 10. Schematic illustrating a senescent haploid yeast cell undergoing fusion with a normal haploid cell to form a diploid. Only one chromosome is shown in each cell. *S. cerevisiae* has a total of 16 chromosomes and shortened ones in the left cell are complemented by undamaged ones in the right one.

To initiate the mating experiment, telomerase-deficient *MAT α est2* cells were streaked on glucose media plates and were allowed to reach a near-senescent phase (three streaks). Cells were then harvested from the third streak and transferred into YPDA liquid media. Equivalent amounts of telomerase-deficient *MAT α est2* cells (YLKL803)

and telomerase-proficient *MAT α* cells (YLKL701) were introduced into YPDA liquid media. After a period of 2 hours of mating, cells were aliquoted in different concentrations onto Petri plates containing diploid selective media.

The genotype of YLKL803 is *MAT α est2 leu2 his3 lys2*, which means that it cannot synthesize leucine, histidine or lysine. Thus, YLKL803 cells cannot grow on plates lacking these three amino acids. The genotype of YLKL701 is *MAT α ade5*, indicating that it cannot synthesize adenine and will not grow on plate media that lacks adenine. YLKL803 x YLKL701 diploids have the following genotype:

MAT α est2 leu2 lys2 his3 ADE5
MAT α EST2 LEU2 LYS2 HIS3 ade5

Unlike the haploids, these diploid cells are able to grow on plates lacking leucine, lysine, histidine and adenine.

Wildtype *MAT α* cells formed diploids after mating with *MAT α* cells (YLKL701) with an efficiency of 22% (Table 2). Under the same experimental conditions, cells that were in a late senescent phase, which had short telomeres and had lost all capability for growth, were rescued by mating to telomerase-expressing YLKL701 cells (Table 2). Mating efficiency was approximately the same for normal *MAT α* cells and for late senescent *MAT α* cells (22% vs. 18%). This again argues that senescence is not an irreversible process, but can be reversed through not only the *EST2* polymerase expression system but also through cell mating.

Table 2.

Mating rescue of telomerase-deficient versus wildtype cells			
Strain	Normal Cell growth	Mating Rescued Cells	Fold Increase
WT	65.8 ± 5.5	21.6 ± 7.0	
<i>est2</i>	0.68 ± 0.36	17.6 ± 3.2	25

The *EST2* reactivation and mating rescue experiments demonstrated that most aged cells do not die immediately after 60-70 generations of growth.

To further explore the viability of senescent cells, a cell holding experiment was conducted to examine the following question: Do senescent cells that have stopped growing lose their ability to be rescued over time or, alternatively, are these cells capable of sitting on a glucose plate for days or weeks not growing, but also not dying? Figure 11 displays how cells reaching senescence were continually held in a 30 °C incubator for eight consecutive days. After every two days, cells were harvested and plated on both glucose and galactose media plates. Cells that were spread on glucose media were not expressing telomerase because the promoter remained off. Since these cells were harvested from the third streak, once spread onto glucose plates they would be capable of very few additional cell cycles. If these cells were spread on galactose plates, telomerase expression would activate and cells would, at least potentially, re-initiate proliferation.

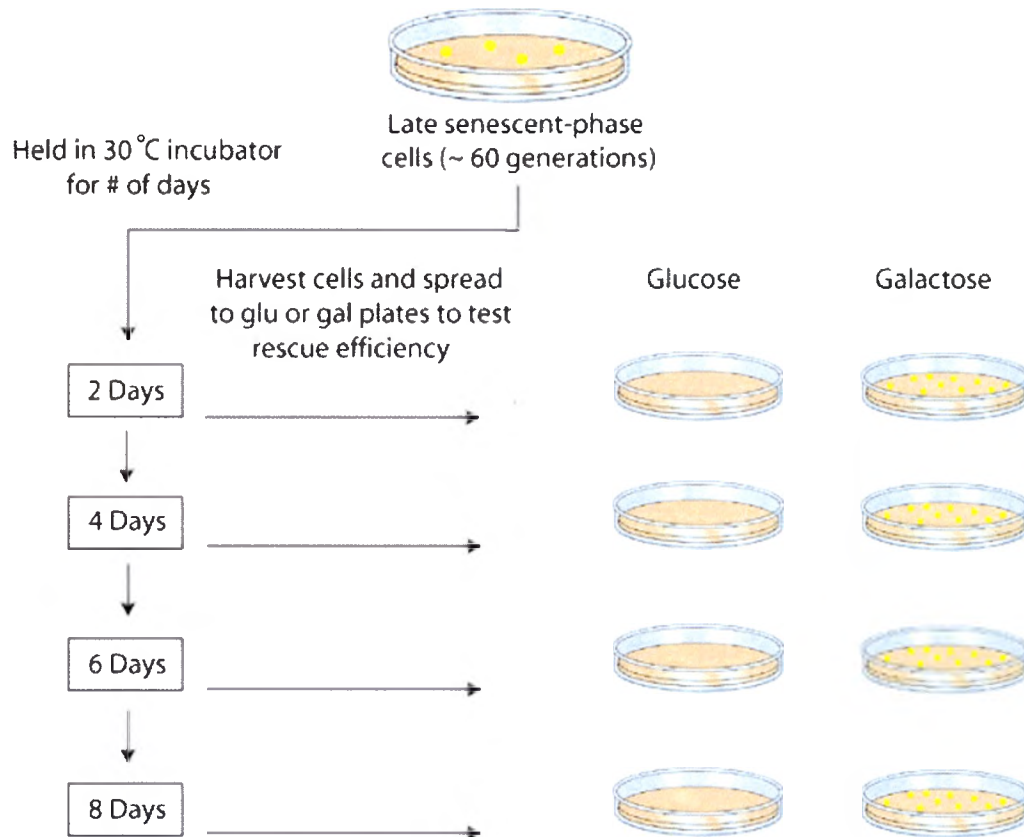


Figure 11. A schematic representation of the holding experiment showing the theorized outcome of senescent cells grown past ~ 60 generations and rescued when plated on either glucose or galactose plates.

Figure 12 presents the results obtained from the holding experiment. Wildtype cells (the control) harvested from the same plate held in the incubator for many days when spread on either glucose or galactose showed a high plating efficiency (~50%) that was maintained for all 8 days. Telomerase-deficient cells continually held on a single glucose plate (telomerase off) were initially rescued by *EST2* reactivation with approximately 25% plating efficiency and this rescue capability decreased only gradually over the next eight days. These results give strong evidence that cells do not actually die

after reaching senescence, but appear to simply arrest growth. The holding experiment implies that cells after reaching a senescence phase continue to metabolize and are still capable of being rescued after a prolonged period of time using the expression system to reactivate telomerase.

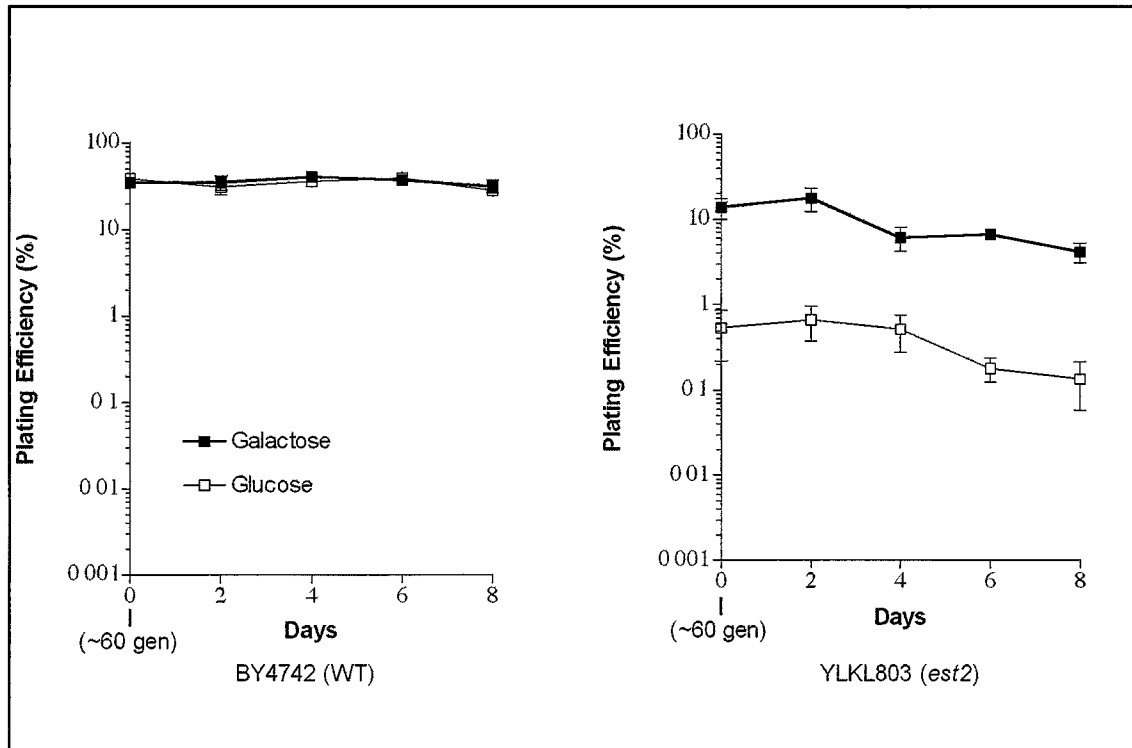


Figure 12. A graph illustrating the percent plating efficiency of wildtype and senescent cells that were continually held in the incubator for eight consecutive days.

In eukaryotes the cell cycle is composed of a series of events that must be fulfilled for completeness. In a cycle the completion of one event is dependent upon an earlier completed event. This dependency is genetically controlled by surveillance mechanisms called checkpoints (25). Checkpoints are activated in response to incomplete processes

in the normal cell cycle and they can also be activated when a cell's chromosomes are damaged by an exogenous agent. The illustration in Figure 13 displays the consequences to normal cells with active checkpoint genes that have been exposed to ionizing radiation. Cultures of eukaryotic cells such as yeast contain a mixture of G_1 , S, G_2 and M phase cells. When these cells have been damaged by radiation they each progress through the cell cycle until they arrest in the G_2 phase. The cells pause in G_2 long enough to repair the induced damage and later resume mitosis when the damage has been repaired.

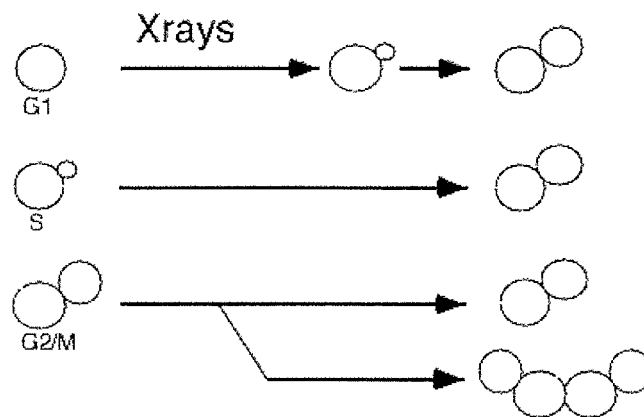


Figure 13. Cultured cells of the budding yeast *S. cerevisiae* arrest cycling after exposure to X-rays, forming dumbbell-shaped G_2 phase cells.

Cultured human and yeast cells lacking telomerase also exhibit a cell cycle checkpoint response. *est2* cell cultures are composed primarily of G_2 phase cells in late senescence. It is likely that this occurs because progressive telomere shortening eventually leads to uncapping of the DNA ends and the cell interprets this as a sign of DNA damage (Figure 14). Several genes have been identified as essential for X-ray damage checkpoint signaling and a subset of these have also been shown to be essential

for senescence-associated cell cycle arrest. As shown in Figure 14 these genes include *MEC1*, *MEC3*, *DDC2*, *RAD9* and *RAD24* (11, 12).

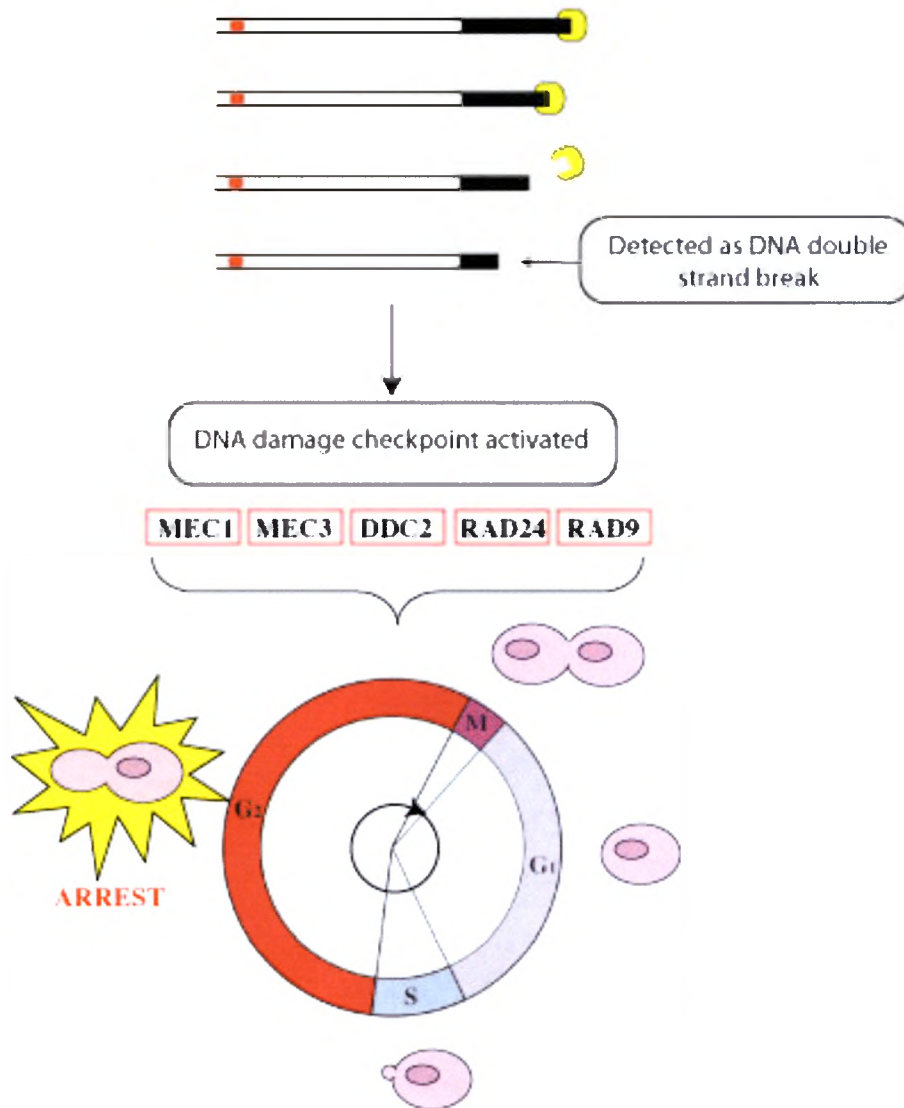


Figure 14. Illustration depicting how telomere erosion leads to loss of the protective protein cap, which is interpreted by the cell as broken (damaged) DNA ends. Such structures then activate the DNA damage checkpoint response system causing cell cycle arrest in G₂ phase.

Since genes involved in the DNA damage response are also involved in telomere length maintenance, experiments employing *S. cerevisiae* checkpoint mutant strains were critical to further analyze the efficacy of cell rescue using the telomerase expression system and also to establish if cells with inactive checkpoint genes were capable of living for as long or near to long period of time even after reaching late senescence. Key genes involved in the checkpoint response in *S. cerevisiae* as mentioned above include *RAD9*, *RAD17*, *RAD24*, *MEC3*, and *DDC1* (Figure 14). These genes are required in order to recognize the presence of damaged DNA and activate the checkpoint response. The checkpoint mutant strains used in this experiment were *mec3 rad24*, and *mec3 rad24* double mutants. An image on Figure 15 depicts the shape cells form when arrested in G_2 phase.

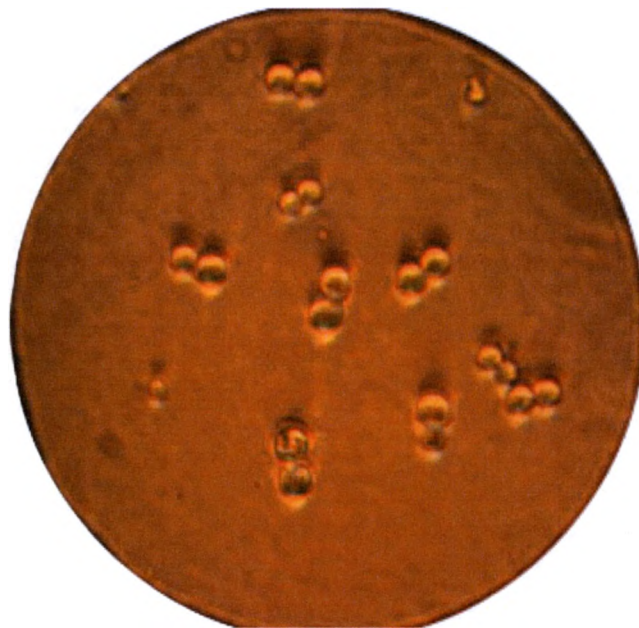


Figure 15. A photograph of senescent, G_2 arrested cells forming the shape of a dumbbell. Cells were visualized using a phase contrast microscope.

The results seen in Figure 16 show a representation of the percent of G₂ arrest occurring in the different mutant strains. Cells harvested from colonies of normal cells (WT) had reached stationary phase and had only 1% G₂/M cells. In contrast, third streak *est2* colonies contained 30% G₂/M cells. Checkpoint mutant strains *est2 mec3*, *est2 rad24* and *est2 mec3 rad24* double mutant were less efficient in arresting in the cycle, exhibiting 12-20% G₂/M cells.

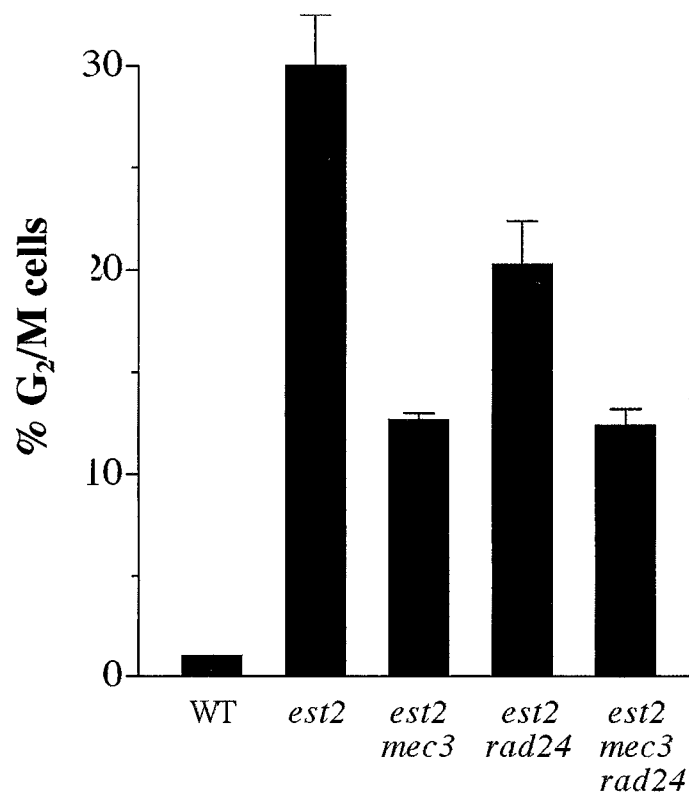


Figure 16. Analysis of the fraction of dumbbell-shaped G₂/M cells (mostly G₂) in colonies formed by wildtype strains and by senescent telomerase-deficient strains with or without inactivated checkpoint genes.

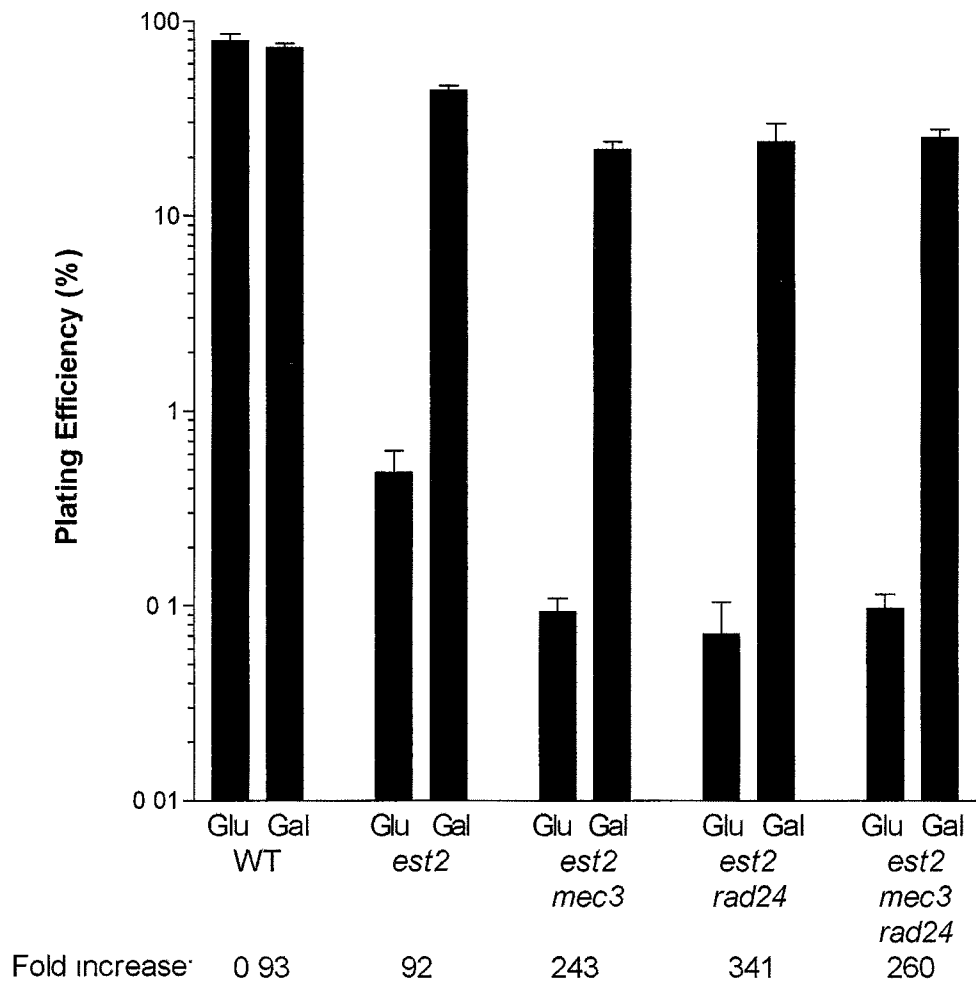


Figure 17. Graph depicting the results of the reactivation experiment. The plating efficiencies of cells grown on glucose plates (*EST2* polymerase remains off) versus galactose plates (*EST2* polymerase is expressed) are displayed. Error bars indicate standard deviations.

To assess the capability of senescent checkpoint mutant cells to restore telomere lengths through the reactivation system, the *GALI-V10p::EST2* reactivation experiment was once again conducted on these strains. The steps of the reactivation experiment can be visualized in Figure 7. *est2 mec3*, *est2 rad24*, and *est2 mec3 rad24* strains were streaked to glucose plates until they had lost the capacity to continue growing. The cells were then harvested, counted and spread onto fresh glucose plates (which keeps the *GALI-V10p::EST2* fusion off) or onto galactose plates (turning *EST2* expression back on).

As shown in Figure 17, 99.9 % of the telomerase-deficient, checkpoint mutant cells were unable to form colonies when telomerase was kept off (on glucose plates). Plating efficiency on glucose was 5-fold lower in the three checkpoint mutants than in cells only deficient in telomerase (*est2*). This suggests that being able to pause cycling conferred some survival advantage onto the checkpoint proficient cells. When these non-growing senescent cells were spread to galactose plates, turning telomerase back on, colony formation was increased 240-340 fold. Compared to *est2* cells, these checkpoint mutant cells were rescued at a similarly high rate (~25% plating efficiency versus 40% for *est2* single mutants). Thus, the reactivation results indicate that checkpoint gene mutant cells were capable of being rescued at a very efficient rate.

The question of prolonged viability was also assessed in the checkpoint mutants. Once again, a holding experiment was performed as shown in Figure 11 to evaluate how long cells remained viable after senescence. Figure 18 below reveals that even if cells are defective in the checkpoint genes and have reduced cell cycle arrest or pausing in G₂ phase, they continue to survive for many days, exhibiting similar plating efficiency to the

checkpoint proficient *est2* cells. These cells continue to be viable for a prolonged period of time and establish that senescence is reversible both short-term and also long-term.

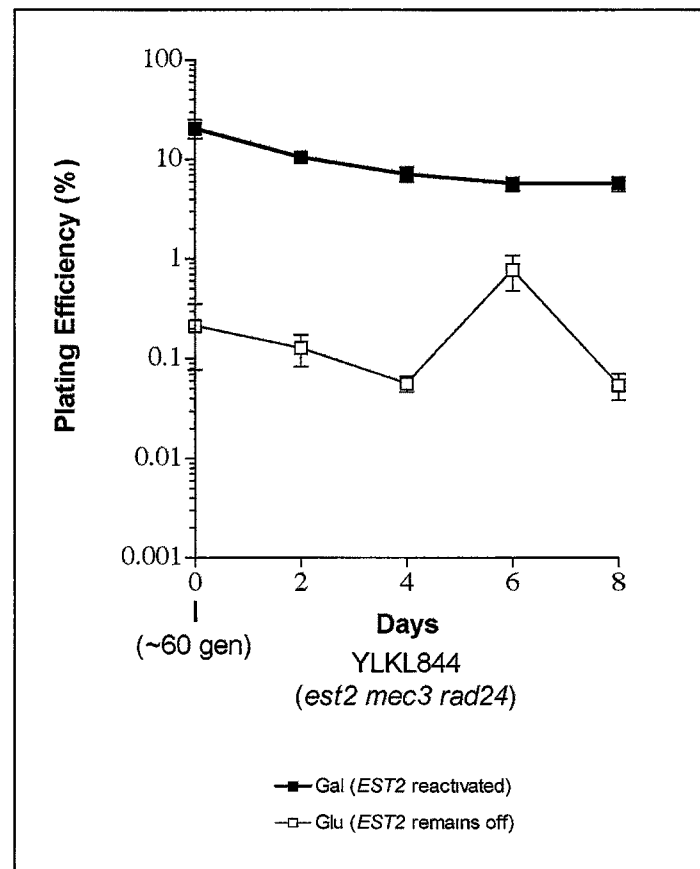


Figure 18. Checkpoint mutants that have undergone senescence and lost growth capability retain the ability to be rescued by telomerase reactivation for up to eight days.

The previous experiment established that most senescent cells were rescuable by reactivation of *EST2* polymerase expression. A critical question was addressed next: does resumption of telomerase synthesis in senescent cells lead to extension of the

critically short telomeres and, if so, do they go back to normal lengths? Analysis of telomere lengths was performed using Southern blots. This technique is routinely used to locate and identify DNA size fragments on a membrane. These fragments are later hybridized with a complementary probe that will reveal the presence of a particular sequence of DNA on the membrane. In our specific experiments DNA samples of wildtype or rescued cells was extracted and digested with *XhoI*. These samples were later and quantified and prepared for gel electrophoresis loading using TE buffer and dye glycerol. Approximately one microgram of digested DNA per well was loaded on 1.2 percent agarose gels. The gel was then electrophoresed and treated with denaturing buffers. The use of these buffers allowed the double stranded DNA on the gel to separate into single strands. Once these strands were separated, the single-stranded DNA was then transferred through capillary action onto a nylon membrane. Once the transfer was completed, the DNA on the membrane was crosslinked by applying a brief period of ultraviolet irradiation. Once the DNA had been crosslinked, a telomere-specific single-stranded DNA probe was introduced on the membrane and allowed to hybridize with the single-stranded DNA on the membrane overnight. Once the hybridization process was complete, an enzyme conjugate antibody was then reacted with the probe on the membrane. The enzyme attached to the antibody converted a chemiluminescent substrate to product plus light. The membrane was then exposed to X-ray film that was later developed to analyze lengths of telomere fragments in different mutant strains. Figure 19 briefly demonstrates the process of Southern blot analysis.

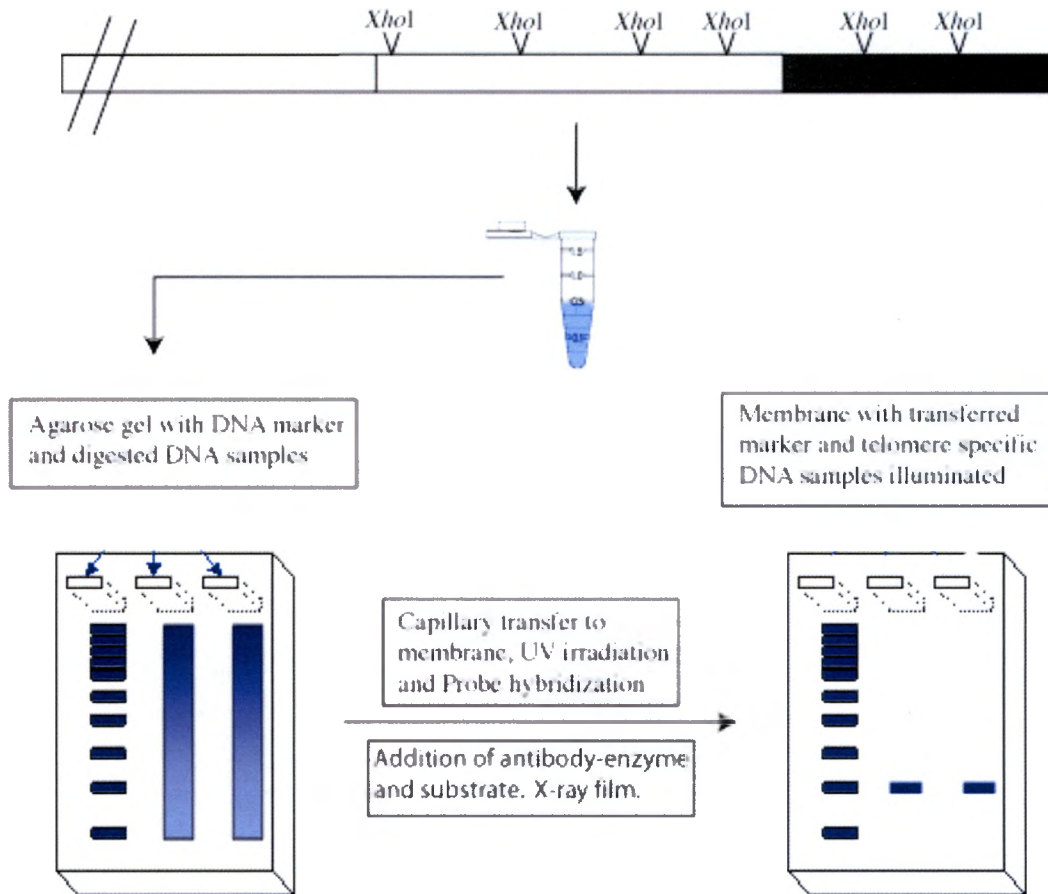


Figure 19. A schematic representation of a Southern blot experiment. This figure illustrates the *XhoI* restriction sites on a chromosome. These sites are digested and the DNA is loaded onto an agarose gel and later transferred to a membrane. After the addition of a telomere-specific probe, an antibody-enzyme conjugate and a substrate, the membrane is placed in a cassette with X-ray film for exposure. The outcome is dark bands on a film demonstrating sizes of telomere specific end fragments (from an *XhoI* site to the end).

Southern blots using telomere-specific probes against *XhoI*-digested DNA produce multiple bands in each lane because yeast cells have 16 different chromosomes

with 32 telomeric ends. Many of these 32 ends have an *XhoI* site approximately 1,200 bp from the terminus and this is why a broad (tall) lowest band is observed at 1,200 bp in DNA from normal cells. The lowest band contains a mixture of many fragments that all have the same *XhoI* end, but vary in lengths of telomere repeats on the other end. Each of the fragments has approximately 800 bp of subtelomeric DNA on one end, next to the *XhoI*-cut end, and 300-400 bp of telomere repeats on the other side, in amounts that are different for each fragment because telomerase does not extend every end the same distance during each S phase of the cell cycle. Degradation of the chromosome will vary among ends as well.

In each Southern blot there are approximately a dozen additional bands above the broad lowest band. These are usually derived from individual ends (not a mixture of ends like the lowest band) that, because of natural variation among chromosomes, do not have the nearby *XhoI* site that is ~ 1,200 bp from the terminus. However, these ends do have recognition sites for *XhoI* at positions that are further away from the terminus. For example, the nearest *XhoI* sites on two yeast chromosome ends are ~2,000 and 2,500 base pairs (bp) from the terminus, respectively, which produce the second and third smallest fragments in the Southern blot in Figure 20. Bands in the Southern blots that are higher than these two fragments are generated from ends that have their closest *XhoI* site even further back from the terminus, producing even larger fragments containing *XhoI*-derived overhangs on one end and a telomere at the other end.

In order to locate and determine telomere lengths of rescued cells, we first had to establish the telomere length of the parental strain, BY4742 (WT). Once these cells had grown on glucose plates in the 30 °C incubator, colonies were harvested, DNA was

purified, digested with *Xho*I, precipitated and loaded (1 μ g) onto a 1.2% agarose gel. To have a reliable estimated length for BY4742, 30 samples (30 different colonies) were tested. Fourteen of the samples tested are represented in the blot shown in Figure 20. The first lane contains molecular weight standards that vary from 947 bp to 21,226 bp. The second lane is control DNA from the parental strain BY4742. The remaining lanes (1-14) demonstrate the 14 samples of BY4742 that were tested. As is visible in Figure 20, the broad, lowest telomere fragment in the control strain (lane C) had an approximate size of 1,150 base pairs (bp). The 14 BY4742 colonies' DNA was similar to the control. In the process of analyzing the results, an interesting observation was made. The second and third smallest fragments in each lane (around 2,000 – 2,500 bp in size) displayed remarkable heterogeneity in size. Similar, but less extensive heterogeneity has also been seen in experiments performed by Cech *et al.* (33). It is likely that the size differences in different isolates of the same strain are due to recombination (strand exchange) events occurring in the cell (discussed in more detail below).

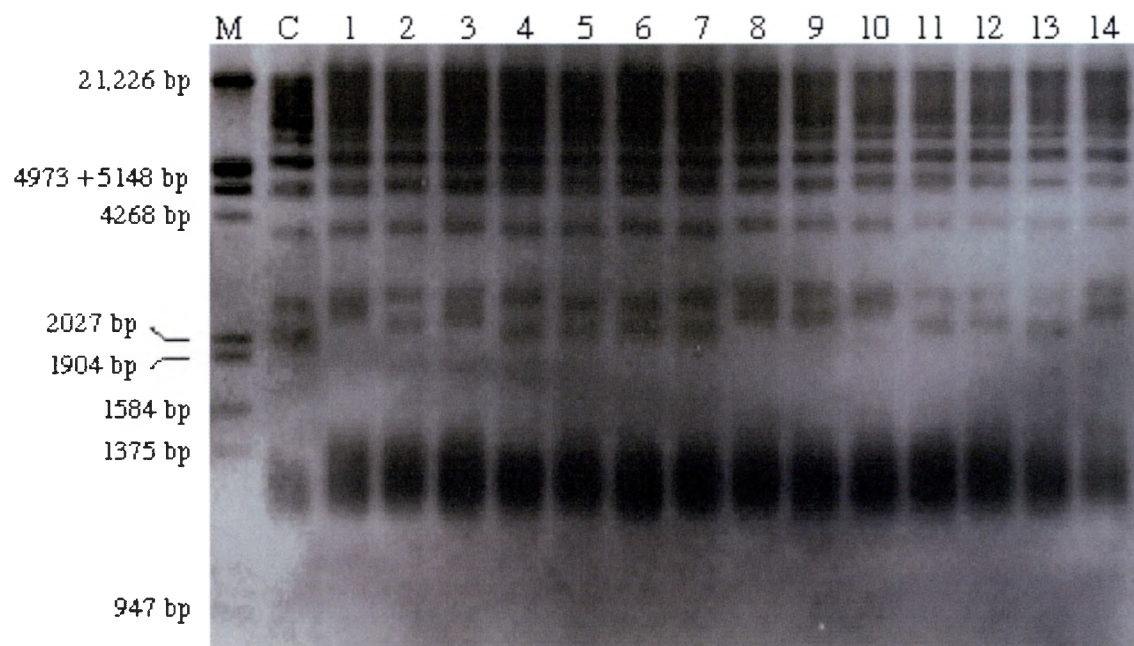


Figure 20. A demonstration of a Southern blot illustrating 14 independent isolates of strain BY4742.

To assess the ability of senescent cells to restore telomere lengths, we first wanted to analyze telomere shortening progression in telomerase-deficient cells. *est2* cells that were streaked in a senescence assay fashion on glucose plates (see Figure 6) were harvested after the completion of every streak (every 3 days). Cells were then introduced into liquid media that would allow the cells to grow to higher density for several hours. This step was necessary for sufficient sample of DNA to be extracted. Following extraction, DNA was digested with *XhoI* and a Southern blot was completed (see Figure 19). As seen in the figure, the terminal telomere fragment length decreased from 1,150 bp to approximately 950 bp over the course of 70 generations of growth (measured using the smallest terminal fragment in each lane).

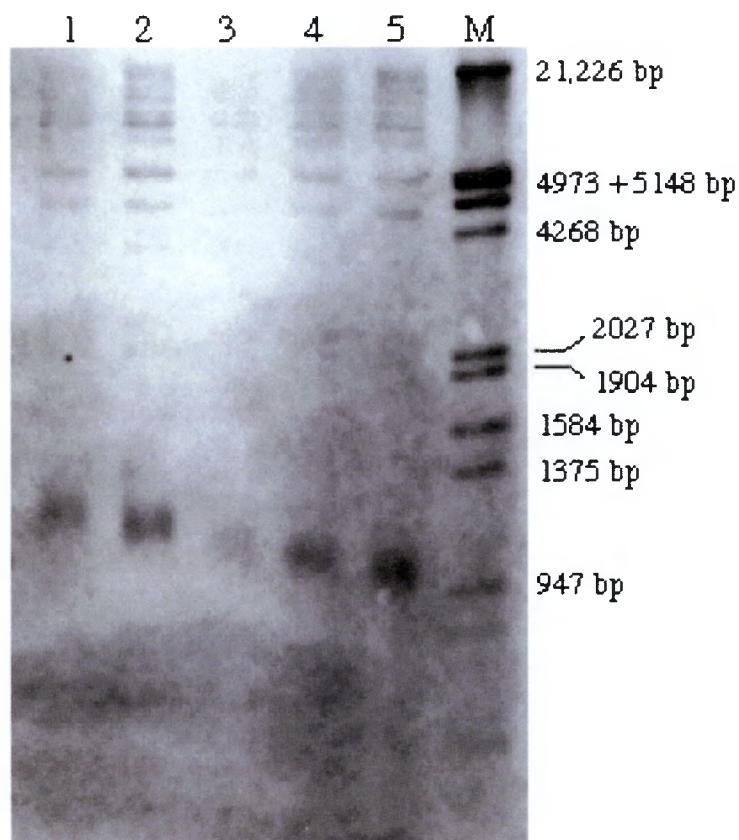


Figure 21. Southern blot representing the progressive telomere shortening that occurs during propagation of a telomerase-deficient strain (YLKL803). Lanes 1-5 correspond to approximately 1, 20, 40, 55 and 70 generations of growth during senescence respectively.

Progressive telomere shortening analysis of a DNA damage checkpoint response mutant strain was also done. Figure 22 depicts the progressive shortening of *mec3 rad24* cells (YLKL844). As seen in this image, shortening of the telomeres also occurred over time, though the ultimate average size (lanes 4 and 5) was not as small as seen in checkpoint-proficient *est2* cells (Figure 21).

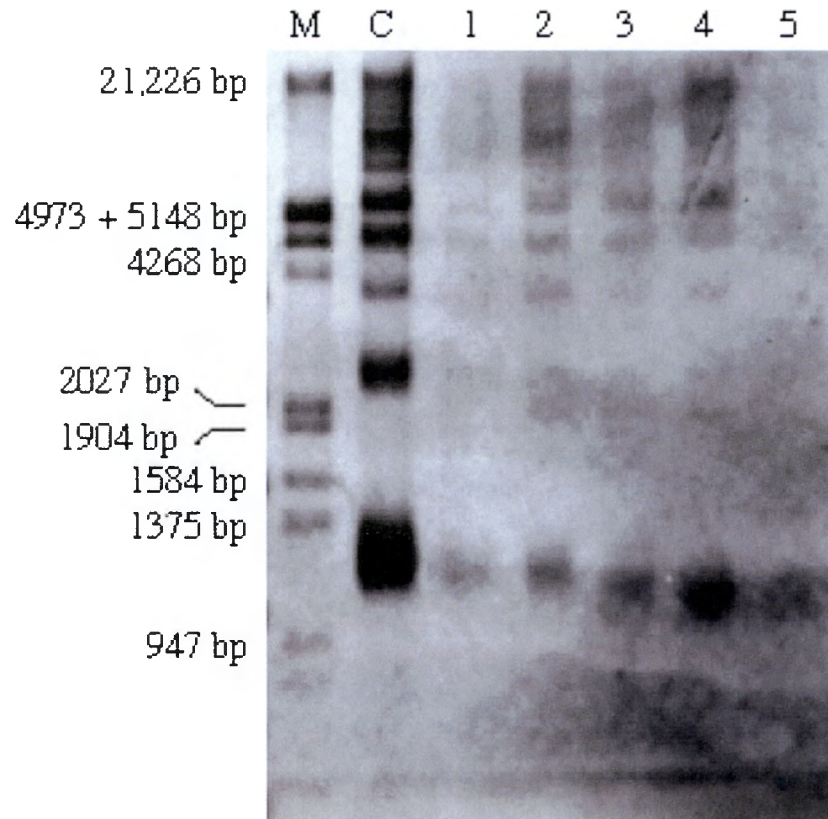


Figure 22. This image depicts the progressive telomere shortening in a checkpoint mutant strain (YLKL844). C, wildtype cell DNA control. Lanes 1-5 correspond to approximately 0, 20, 40, 55 and 70 generations.

After telomerase-deficient (*est2*) cells were rescued using the Est2 polymerase expression system, individual rescued colonies were harvested from galactose plates (Est2 polymerase synthesis on) and DNA was extracted. The DNA was digested with *XhoI* and Southern blots were performed as before. A total of 30 samples were analyzed. Figure 23 illustrates DNA from 5 BY4742 colonies (lanes 2-6) and 5 *est2* rescued isolates (lanes 7-11). Size differences between these two strains can be observed. Figure 24 shows DNA from 12 colonies (lanes 1-12) that were rescued using the expression system.

This Southern blot image demonstrates that all of the rescued cells had near-normal telomere lengths, i.e. compared to the control (BY4742), the rescued cells almost fully restore the telomere lengths. Interestingly, several isolates had completely lost one or more band. This phenomenon was not seen in the 30 control DNAs analyzed in both Figure 20 and 21.

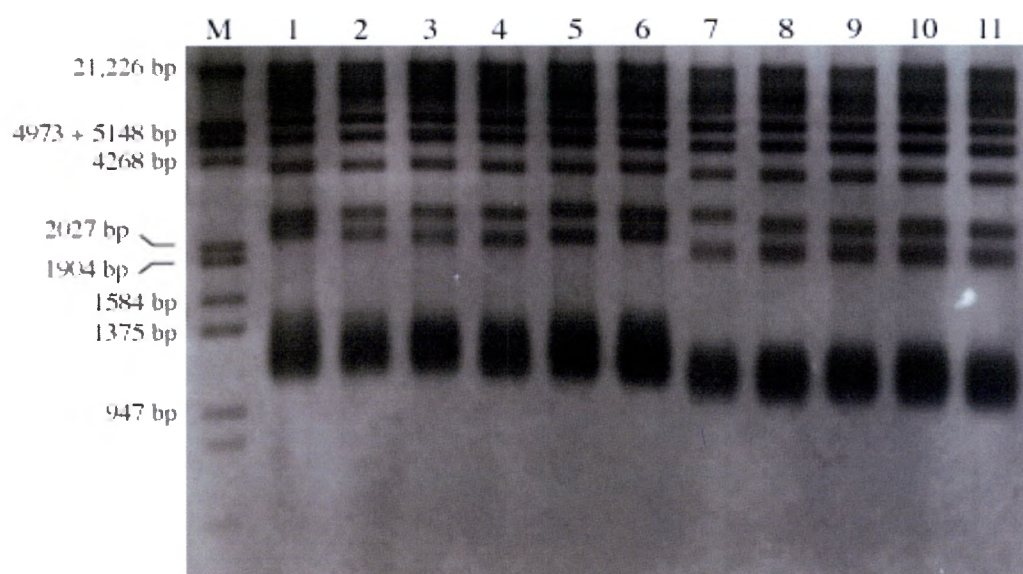


Figure 23. Southern blot demonstrating fragment sizes of five BY4742 isolates (lanes 2-6) and five rescued *est2* isolates (lanes 7-11).

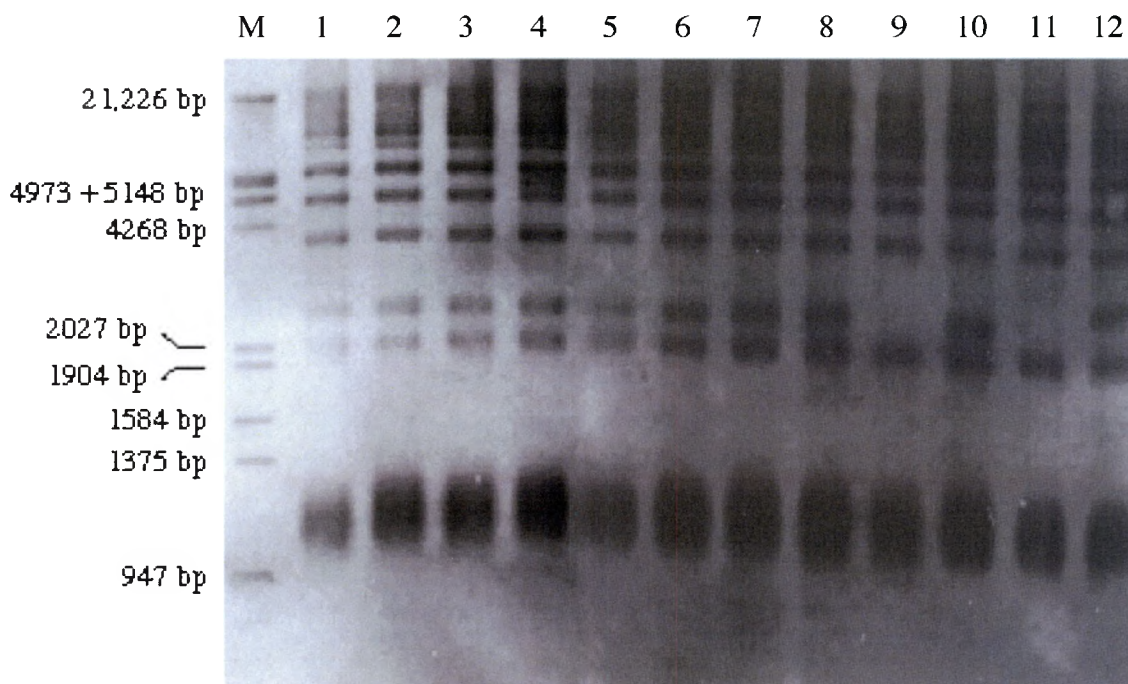


Figure 24. Southern blot image of terminal telomere DNA fragments from rescued *est2* cells.

We also analyzed the chromosome lengths of rescued telomerase-deficient checkpoint double mutant YLKL844 (*est2 mec3 rad24*). A total of 34 samples were analyzed, and 14 are shown on Figure 25. After the reactivation of telomerase in the checkpoint double mutants, the telomeres were also restored (lanes 1-14), but, as before, were not quite the same lengths as the parent strain BY4742 (control). As in the rescued *est2* cells, several isolates exhibited missing bands.

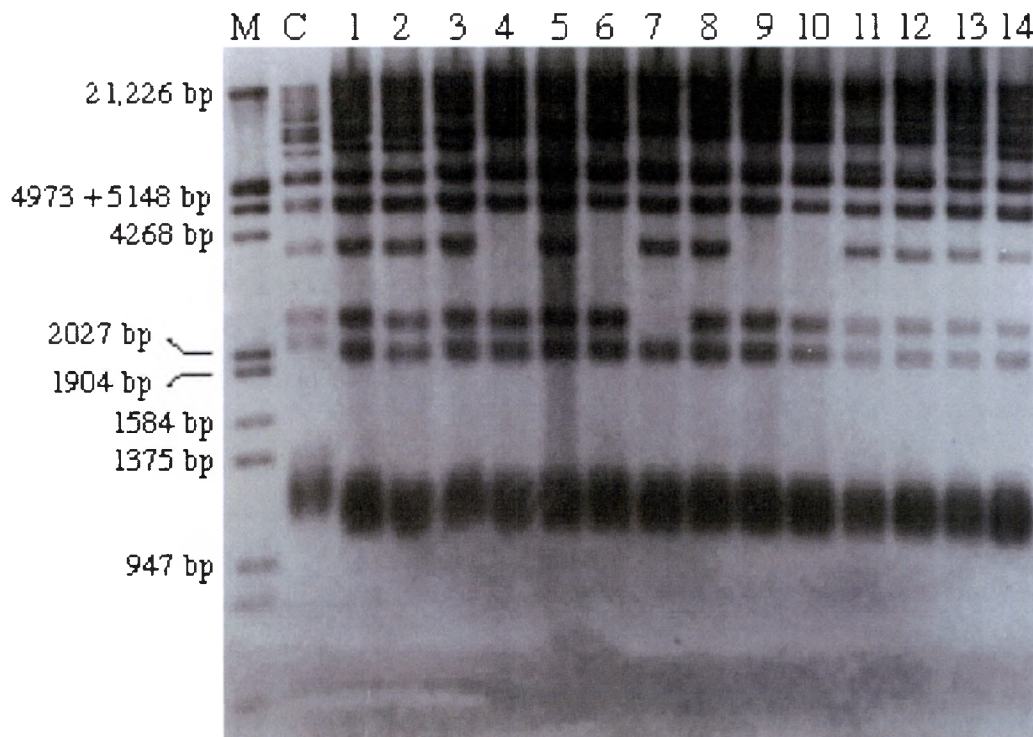


Figure 25. A Southern blot illustration of *est2 mec3 rad24* (YLKL844) rescued telomere lengths compared to the telomerase-proficient strain (BY4742).

Finally, a last Southern blot was performed to also analyze telomere lengths in recombination-deficient YLKL807 (*rad52*) cells that had also been rescued through the Est2 polymerase expression system. Analysis of 30 rescued colonies was performed and 17 are shown on Figure 26. Similar to the other rescued mutant cells, chromosome ends were also restored to near-normal lengths in the *est2 rad52* cells. The slight curvature of the lanes in Figure 26 is a gel electrophoresis artifact. Interestingly, the smaller bands did not exhibit variation. In BY4742 (WT), *est2* mutant and *est2 mec3 rad24* double mutants, size variations or lost bands were observed, but not in *rad52* mutants. Since *RAD52* is essential for homologous recombination to occur, having a mutation in this

gene would theoretically lead to reduced strand exchange between chromosomes. This lack of telomere-telomere recombination also is likely to be the reason that *est2 rad52* mutants show greater loss of viability during senescence (23, 27).

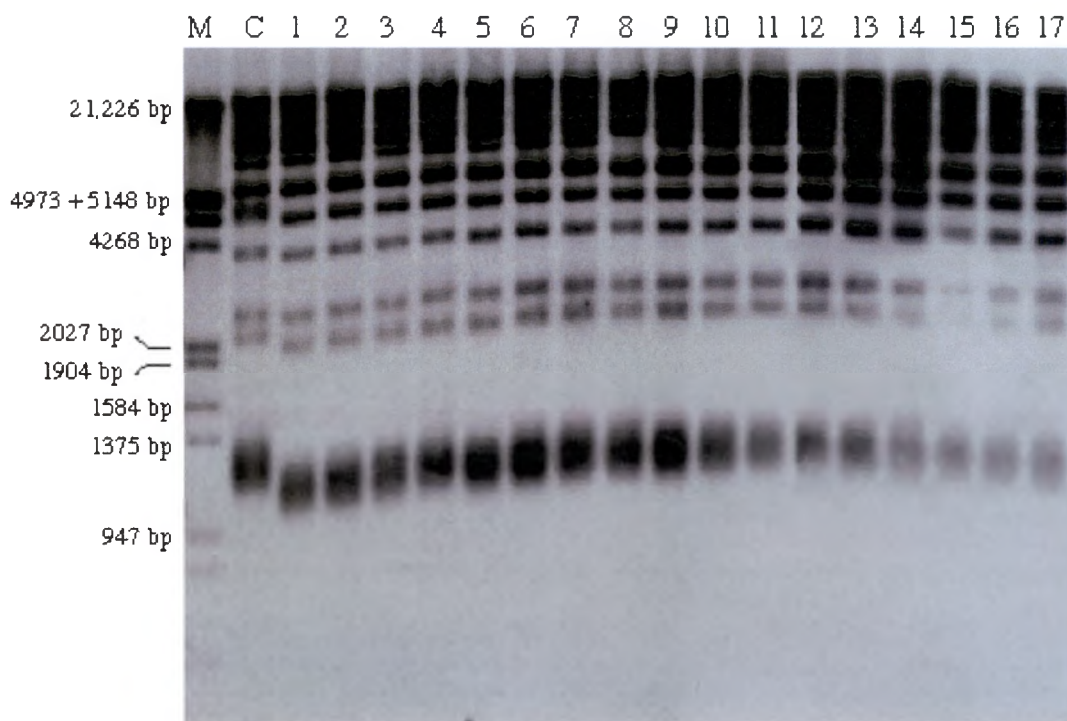


Figure 26. Southern blot analysis of DNA from rescued *est2 rad52* (YLKL807) mutants.

Table 3 represents the size variation between the 2,000 – 2,500 bp fragments and the number of missing or added fragments in BY4742, *est2*, *est2 mec3 rad24* and *est2 rad52* cells. The total number of isolates that either had a size variation or a missing band were quantified from all isolates that were tested.

Table 3. Variation in number of telomere fragments and lengths of the two ~ 2,000-2,500 bp bands

Strain	<u>2nd and 3rd band size variation</u>		Gain/Loss of <i>Xho</i> I sites
	Upper	Lower	
BY4742 (wildtype)	8/31	15/31	0/31
<i>est2</i> (rescued)	4/30	1/30	6/31
<i>mec3 rad24</i> (rescued)	0/28	0/29	5/29
<i>rad52</i> (rescued)	0/33	0/33	0/33

Examination of telomere lengths in 30 different isolates (colonies) of wildtype cells revealed frequent size variation among the 2nd and 3rd lowest fragments (approximately 2,000 and 2,500 bp in size). This phenomenon has been observed before (e.g., 10, 33) and is caused by variation of lengths at the telomeric ends of each fragment. For example, all of the 2nd smallest fragments in each lane in Figure 20 have the same *Xho*I-cut end, but vary in length on the telomere-proximal side. The DNA loaded in each lane was purified from >10⁸ cells taken from a single colony on a plate, yet each isolate produced only one 2nd lowest band and one 3rd lowest band that was frequently slightly larger or slightly smaller than in the original parent strain. This movement of one of the bands to a new location, without seeing a band of the original size present as well, indicates that each of these upper bands is likely to be derived from only one chromosome end and that the alteration in size was stably inherited among most cells in the colony. Put another way, the new location of each band in the lane, higher or lower,

indicates a stably inherited alteration in size of that particular chromosome end in the cells. In contrast, the slight variations in thickness (height from bottom to top) of each band are caused by the fact that they are made up of many individual fragments whose exact number of telomere repeats varies slightly because telomerase synthesis, as well as DNA degradation processes, vary from cell to cell at individual ends.

The ~2,000 and 2,500 bp bands (2nd and 3rd-lowest bands in each lane) exhibited size alterations frequently in DNA isolated from different colonies of wildtype cells and also in different colonies containing rescued *est2* cells (Table 3). In contrast, no alterations of these two bands were observed in any of the rescued *rad52* mutants or rescued *mec3 rad24* checkpoint mutant cells. Rad52 protein is essential for strand exchange (homologous recombination) between independent chromosomes and also between sister chromatids (24). The prevalence of altered bands in *RAD52* cells (recombination-proficient) and the absence of variation in *rad52* mutants suggests that the size changes are caused by unequal strand exchange events between subtelomeric and telomeric DNA regions of two chromosome ends. These exchanges might theoretically be between the ends of two different chromosomes, which may or may not have identical *XhoI* recognition sites, or they might occur between duplicated sister chromatids, which are identical in sequence and have the same distribution of *XhoI* sites at each end. We did not observe any missing *XhoI* fragments among 31 isolates of wildtype cells, which would be produced if recombination occurred between different chromosomes (e.g., from gene conversion events that add or remove *XhoI* sites to change the distribution of such sites on one end to be the same as those on another chromosome's end). This observation suggests that most naturally occurring size variation in these bands in wildtype cells is

caused by sister chromatid exchange events that are subsequently stably passed on from one cell to the next. The lack of such altered bands in *mec3 rad24* double mutants appears to support this idea. Cells lacking the checkpoint protein Rad9 have been shown to be strongly defective in Xray- and HO endonuclease-induced sister chromatid exchange (35). If cells lacking the checkpoint proteins Mec3 and Rad24 have the same defect, then, like *rad52* cells, they would not exhibit variations in size in telomere fragments and that is what we observed (Table 3).

Additional to the variation among bands, missing fragments in rescued *est2* cells (Figure 24 lanes 9 and 11) and *est2 mec3 rad24* cells (Figure 25 lanes 4,6,7,9 and 10) was observed. This, however, was not observed in either wildtype (Figure 20) or *est2 rad52* (recombination-defective) cells (Figure 26) which hints that the cause of this phenomenon is possibly due to interchromosomal recombination events since we observed no missing or added fragments in *est2 rad52*. This is indicative that the active recombination gene *RAD52* may influence the presence or lack of fragments. A large possible cause of this phenomenon is that these events might have been stimulated due to extensive chromosomal degradation. In homologous recombination, a repetitive sequence on a chromatid may not line up exactly with its corresponding region in a homologous chromatid, for example in *XhoI* sites, and may result in unequal recombination. If interchromosomal recombination is stimulated by extensive chromosomal degradation, this could eventually lead to a deletion or even possibly addition of *XhoI* sites, appearing on a Southern blot membrane as either missing bands or added bands as seen on Figure 24 and 25.

SUMMARY AND CONCLUSIONS

The expression system used in these experiments has allowed testing of several models for cell aging. Both the *Est2* expression system and the mating rescue experiments demonstrated that cell growth arrest during senescence is not an irreversible process. This result implies that three of the four major models of senescence are incorrect. These models include proposals that senescence is a process that occurs due to lethal chromosome rearrangements such as end-to-end chromosome fusions, that nucleases play a role in degradation of DNA into internal essential genes within chromosomes, or that the cell is triggered into a programmed cell death (apoptosis). An alternative model that we propose is that cells simply arrest growth and continue to metabolize nutrients in much the same way that normal stationary phase cells do.

Additionally the holding experiment established that senescent cells have the capacity of prolonging their life by simply arresting growth in G_2 phase of the cell cycle. Cells remain viable and can be rescued over a period of many days and therefore do not undergo irreversible, lethal events, even long after growth has ceased.

Analysis of telomere-deficient, DNA damage response checkpoint mutants reinforced the conclusion that senescent cells are not committed to irreversible death due to telomere damage. These checkpoint mutants, however, did exhibit a reduced ability to arrest in G_2 and did demonstrate a slight increase in cell death when compared to *est2* cells that were checkpoint-proficient.

Southern blots confirmed that telomeres shortened progressively with increasing generation time in *est2* and *est2 rad24* mutants. Furthermore, they revealed that rescued

est2, *est2 rad52* and *est2 mec3 rad24* cells had restored their short telomeres back to near-normal lengths (i.e., similar to those of the parental strain BY4742).

As observed in a previous study (33), randomly picked colonies of normal cells displayed remarkable variation in the sizes of some of their telomere fragments. One possibility is that this variation is due to high rates of strand exchange between the highly homologous sub-telomeric and telomere regions of chromosomes. This concept was supported by the finding that rescued senescent *rad52* mutants, which are recombination-defective, did not exhibit such subtle variation in size. This finding explains why other telomerase-deficient strains lacking checkpoint genes, but which had functioning recombination genes, also demonstrated variation in their telomere fragments.

It was notable that DNA from rescued *est2* and checkpoint-deficient *est2* cells had lost some of the fragments normally seen in Southern blots performed with DNA from wildtype (*EST2*) cells. This finding suggests that severe shortening and nuclease degradation that occurred during senescence sometimes lead to aberrant recombination events between chromosome ends, eventually resulting in the loss of *XhoI* sites that were probed in the Southern blots. These completely missing bands were not seen in rescued *rad52* mutants, which also exhibited much greater cell death because of the deficiency in the recombination pathway. This suggests that chromosome ends that endured strong degradation caused by nucleases needed recombination to restore their ends back to normal, but this was not possible in the *rad52* cells, and so these cells exhibited an increased death rate.

This project has studied aging of cells in cell culture and demonstrated that progressive telomere shortening leads to growth impairment, but not outright death of the

cells. Telomere-shortening occurs in human and animal tissues *in vivo*, and appears to mimic many of the phenotypes seen in cultured senescent cells (34), but its precise consequences remain unknown. Results presented here suggest that cells of elderly humans that have shortened telomeres are likely to have lost the ability to proliferate, and aberrant strand exchange events at the telomeres may be increased, but the cells are not irreversibly compromised and destined to die. Reactivation of telomerase expression in humans (aged or not), as done here with cultured cells, might have beneficial effects, e.g., increased ability of cells to proliferate, but might also come with a price because of possible increased risk for cancer.

REFERENCES

1. Levy, M.Z. *J. Mol. Biol.* **1992**, 225, 951-960.
2. Hahn, W.C. Myerson, M. *Ann Med.* **2001**, 33, 123-129.
3. Lowell, J.E.; Pillus, L. *Cell Mol Life Sci.* **1998**, 54, 32-49.
4. Cawthon, R.M.; Smith, K.R.; O'Brien, E.; Sivatchenko, A.; Kerber, R.A. *Lancet.* **2003**, 361, 393-395.
5. Epel, E.S.; Blackburn, E.H. *PNAS. U.S.A.* **2004**, 101, 17312-17315.
6. Rowley, P.T.; Tabler, M. *Anticancer Res.* **2000**, 20, 4419-4429.
7. Hackett, J.A.; Feldser, D.M.; Greider, C.W. *Cell.* **2001**, 106, 275-286.
8. Lowell, J.E.; Roughton, A.I.; Lundblad, V.; Pillus, L. *Genetics.* **2003**, 164, 909-921.
9. Smogorzewska, A.; de Lange, Titia. *Annu. Rev. Biochem.* **2004**, 73, 177-208.
10. Lundblad, V. *Oncogene.* **2002**, 21, 522-531.
11. Enomoto, S.; Glowczewski, L.; Berman, J. *Mol Biol Cell.* **2002**, 13, 2626-2638.
12. Ijma, A.S.; Greider, C.W. *Mol Biol Cell,* **2003**, 14, 987-1001.
13. Ducray, C.; Pommier, J.P.; Martins, L.; Boussin, F.D.; Sabatier, L. *Oncogene.* **1999**, 18, 4211-4223.
14. Hayflick, L. *Exp Gerontol.* **2003**, 38, 1231-1241.
15. van Steensel, B.; Smogorzewska, A.; de Lange, T. *Cell.* **1998**, 92, 401-413.
16. Wright, W.E.; J.W. Shay. *Nat Biotechnol.* **2002**, 20, 682-688.
17. Dugan, L.L.; Quick, K.L. *Sci. Aging Knowl. Environ.* **2005**, (26) pp.pe20.

18. Beckman, K.B.; Ames, B.N. *Phys Rev.* **1998**, 78, 547-581.
19. Ames, B.; Chen, Q. *Cell Biology.* **1995**, 92, 4337-4341.
20. Chen, Q.; Fischer, A.; Reagan, J.D.; Yan, L.; Ames, B.N. *Proc. Natl. Acad. Sci.* **1995**, 92, 4337-4341.
21. Yokoo, S.; Furumoto, K. *J. Cell Biochem.* **2004**, 93, 588-597.
22. Serra, V.; von Zglinicki, T. *J. Biol Chem.* **2003**, 278, 6824-6830.
23. Le, S.; Moore, J.K.; Haber, J.E.; Greider, C.W. *Genetics.* **1999**, 152, 143-152.
24. Lewis, L.K.; Kirchner, J.M.; Resnick, M.A. *Mol Cell Biol.* **1998**, 18, 1891-1902.
25. Foiani, M.; Pelliccioli, A.; *Mut. Research.* **1999**, 451, 187-196.
26. Chahwan, C.; Nakamura, T.M. *Mol Cell Biol.* **2003**, 18, 6564-6573.
27. Thambugala, H. *Use of a New Regulatable Telomerase Expression System to Monitor In Vitro Cell Aging and the Effects of DNA Damage on Replicative Senescence*, Master's Thesis. **2005**, 10-20.
28. Brachmann, C.B.; Davies, A.; Cost, G.J.; Caputo, E.; Li, J.; Hieter, P.; Boeke, J.D. *Yeast.* **1998**, 14, 115-116
29. Gottschling, D.E.; Singer, M.S. *Science.* **1994**, 266 (5184). 404-409.
30. Avery, A.M.; Willets, S.A.; Avery, S.V. *Journal of Biol Chem.* **2004**, 279, 46652-46658.
31. Grant, C.M. *Molecular Microbiology.* **2001**, 39, 533-541.
32. Hartwell, L.H. *Genetics.* **2000**, 683.
33. Cech, T.R.; Linger, J. *Science.* **1997**, 276, 561-567.
34. Herbig, U.; Jeyapalan, J.C.; Ferreira, M. *Mech. Ageing Dev.* **2007**, 128, 36-44.
35. DeMase, D.; Zeng, L.; Cera, C.; Fasullo, M. *DNA Repair.* **2005**, 4, 59-69.

VITA

Sandra Carolina Becerra was born in Veracruz, Veracruz Mexico on May 14, 1981, the daughter of Maricela Alaniz and Eliseo Alaniz. After completing her work at William Howard Taft High School, San Antonio, Texas in 2000. She entered Texas State University-San Marcos and majored in Microbiology with a minor in Biochemistry. She received a Bachelor of Science degree from Texas State University-San Marcos in August 2005. From there she began graduate school during the fall of 2005 in the Department of Chemistry and Biochemistry at Texas State.

Permanent Address: 8318 Timber Bough
 San Antonio, TX 78250

This thesis was typed by Sandra Carolina Becerra.